Title

A novel head-fixed assay for social touch in mice uncovers aversive responses in two autism models.

Authors

Chari, Trishala
Hernandez, Ariana
Portera-Cailliau, Carlos

Publication Date

2023-09-04

DOI

10.1523/jneurosci.0226-23.2023

Peer reviewed

A novel head-fixed assay for social touch in mice uncovers aversive responses in two autism models.

Trishala Chari[1,2], Ariana Hernandez[1], and Carlos Portera-Cailliau[1,3,*]

[1]Department of Neurology

[2]Neuroscience Interdepartmental Program

[3]Department of Neurobiology

David Geffen School of Medicine at the University of California Los Angeles

Los Angeles, CA 90095

*Lead contact: cpcailliau@mednet.ucla.edu - 710 Westwood Plaza, Los Angeles, CA 90095

ACKNOWLEDGEMENTS

We are grateful to Gunvant Chaudhari for writing MATLAB scripts to detect ball motion, Will Zeiger and Nazim Kourdougli for help with the design of the behavioral apparatus. Kimberly Battista (https://www.battistaillustration.com) made the illustration in Fig. 1a. This work was supported by the following grants: R01NS117597 (NIH-NINDS), R01HD108370 and R01HD054453 (NIH-NICHD), Department of Defense (DOD, 13196175) awarded to C.P-C, Training in Neurotechnology Translation T32NS115753 (NIH), F31HD108043 (NIH/NICHD), and a graduate student fellowship from the Achievement Rewards for College Scientists Foundation to T.C., and the CARE Fellows Program to A.H.

CONFLICT OF INTEREST

We declare that we have no competing interests.

ABSTRACT

Social touch, an important aspect of social interaction and communication, is essential to kinship across animal species. How animals experience and respond to social touch has not been thoroughly investigated, in part due to the lack of appropriate assays. Previous studies that examined social touch in freely moving rodents lacked the necessary temporal and spatial control over individual touch interactions. We designed a novel head-fixed assay for social touch in mice, in which the experimenter has complete control to elicit highly stereotyped bouts of social touch between two animals. The user determines the number, duration, context, and type of social touch interactions, while monitoring an array of complex behavioral responses with high resolution cameras. We focused on social touch to the face because of its high translational relevance to humans. We validated this assay in two different models of autism spectrum disorder (ASD), the *Fmr1* knockout (KO) model of Fragile X Syndrome and maternal immune activation mice. We observed higher rates of avoidance running, hyperarousal, and aversive facial expressions (AFEs) to social touch than to object touch, in both ASD models compared to controls. *Fmr1* KO mice showed more AFEs to mice of the same sex but whether they were stranger or familiar mice mattered less. Because this new social touch assay for head-fixed mice can be used to record neural activity during repeated bouts of social touch it could be used to uncover underlying circuit differences.

SIGNIFICANCE STATEMENT

Social touch is important for communication in animals and humans. However, it has not been extensively studied and current assays to measure animals' responses to social touch have limitations. We present a novel head-fixed assay to quantify how mice respond to social facial touch with another mouse. We validated this assay in autism mouse models since autistic individuals exhibit differences in social interaction and touch sensitivity. We find that mouse models of autism exhibit more avoidance, hyperarousal, and aversive facial expressions to social touch compared to controls. Thus, this novel assay can be used to investigate behavioral responses to social touch and the underlying brain mechanisms in rodent models of neurodevelopmental conditions, and to evaluate therapeutic responses in preclinical studies.

Keywords: autism spectrum disorder, avoidance, head-fixed behavior, facial expression, fragile X syndrome, maternal immune activation, tactile defensiveness, whisker.

INTRODUCTION

Across animal species and humans, social touch is an important component of social interaction and communication that allows for the development of strong kinship bonds (Adolphs, 2009; Dunbar, 2010; Bales et al., 2018). Touch may be experienced under different contexts, such as between parent and offspring, siblings, friends, or even strangers (Chen and Hong, 2018). Whether animals experience social touch as pleasant or aversive, and the degree to which their behavioral responses differ from those related to touching inanimate objects is largely unknown. Moreover, the neural circuits encoding social touch or how activity within those circuits relates to the behavioral repertoire animals exhibit in response to social touch are not fully understood.

Animal studies have begun to address these questions, especially in rodents, using a variety of behavioral paradigms. Unfortunately, the social touch assays currently available have certain limitations. Those that favor naturalistic interactions in freely moving rodents lack temporal and spatial control over individual touch interactions and typically the data collected reflects a mix of different interactions occurring simultaneously (e.g., anogenital sniffing, whisker-whisker contact, allo-grooming) (Bobrov et al., 2014; Lenschow and Brecht, 2015; Mosher et al., 2016; Jennings et al., 2019; Yu et al., 2022). Head-fixed social interaction assays do exist and can allow for the experimenter to track complex behaviors while recording neural activity; however, recent assays lack control over the duration and type of interaction the mouse engages in because one mouse is anesthetized or the interaction occurs only once (Resendez et al., 2020; Jeon et al., 2023). To overcome these problems, we sought to design a novel head-fixed social touch behavioral assay for rodents, in which we could control the duration, number, context, and type of social touch interactions with high precision, while at the same time monitoring an array of complex behavioral responses (facial expressions, pupillary changes, locomotion, etc.) using high frame rate cameras (**Fig. 1**). We focused on a single type of social touch interaction (face-to-face), as opposed to the equally prevalent anogenital sniffing interactions in mice (Chen and Hong, 2018; Ebbesen and Froemke, 2022), because we felt it had more translational relevance

to humans. We took care to ensure that the experimenter had complete control to directly elicit highly stereotyped bouts of social touch between animals.

To validate our new assay, we used it to identify differences in behavioral responses to social touch in mouse models of autism spectrum disorder (ASD). ASD is a prevalent neurodevelopmental condition characterized by deficits in social interaction, repetitive behaviors, and differences in sensory processing (Robertson and Baron-Cohen, 2017). The change in quality of life in autistic individuals is primarily attributed to social deficits, which can be associated with (or even triggered by) atypical processing of sensory stimuli (Baron-Cohen and Belmonte, 2005; Thye et al., 2018; Lee Masson et al., 2019). Apprehension to social touch in ASD could be caused by tactile hypersensitivity (Cascio et al., 2008; Green and Ben-Sasson, 2010; Green et al., 2015; He et al., 2017), which is a strong predictor of future social deficits (Green et al., 2018). Avoidance of social touch by ASD children could prevent them from forming social relationships as adults (Foss-Feig et al., 2012; Thye et al., 2018). In certain rodent models of autism, tactile sensitivity and social interaction deficits also appear to be linked (Orefice et al., 2016), and, in some cases, differences in the development of primary somatosensory cortex (S1) are associated with social deficits (Choi et al., 2016; Reed et al., 2020). Thus, further research into social touch in ASD models is warranted.

We tested two distinct mouse models of ASD (the *Fmr1* knockout model of Fragile X Syndrome – FXS and maternal immune activation mice) in our novel head-fixed social touch assay. We quantified various behavioral responses in the test animal during social touch with a stranger mouse. We observed increased avoidance, hyperarousal (pupil dilation), and more aversive facial expressions (AFEs) to social touch in both ASD models compared to their healthy controls. Furthermore, we found that *Fmr1* KO mice showed greater avoidance and AFEs to forced social touch (with familiar or stranger mice) than wild type controls, but less so to mice of the opposite sex. Our results suggest that this new social touch assay can parse out maladaptive

behavioral responses to social touch in ASD mouse models and might be of use to the larger neuroscience community.

MATERIALS AND METHODS

EXPERIMENTAL DESIGN DETAILS

Animals

Male and female C5BL/6 mice at postnatal day 60-90 on the day of behavioral testing were used for behavioral experiments and were derived from the following mouse lines based on prior publications: wildtype (WT) B6J (JAX line 000664), *Fmr1* KO (JAX line 003025), and wild-type B6NTac (Taconic line) (The Dutch-Belgian Fragile Consortium, 1994; Choi et al., 2016; He et al., 2017; Kentner et al., 2019; Reed et al., 2020). The group/genotypes used for behavioral testing are as follows: WT and *Fmr1* KO mice (JAX line) and PBS and maternal immune activation (MIA) mice (Taconic line). Mice were group-housed with access to food and water *ad libitum* under a 12 hour light cycle (12 hours light/12 hours dark) in controlled temperature conditions. All experiments were done in the light cycle and followed the U.S. National Institutes of Health guidelines for animal research under an animal use protocol ARC #2007-035 approved by the Chancellor's Animal Research Committee and Office for Animal Research Oversight at the University of California, Los Angeles.

Maternal immune activation (MIA)

We followed established protocols (Estes and McAllister, 2016; Kentner et al., 2019). Wildtype B6NTac pregnant dams were injected intraperitoneally with polyinosonic:polycytidylic acid (Poly(I:C)) for MIA or with phosphate buffered saline (PBS; control) at embryonic day 12.5 (E12.5). A small blood sample of the dams was collected from the submandibular vein 2.5 h after

injection and centrifuged to isolate serum. Serum was run through an interleukin-6 (IL-6) enzyme-linked immunosorbent assay (ELISA) kit (Invitrogen). Successful immune activation in Poly(I:C) injected dams was confirmed by demonstrating significantly elevated levels of interleukin 6 (IL-6) in the dams compared to PBS-injected dams (Garay et al., 2013).

Characterization of MIA model

To first characterize the MIA model, we tested whether progeny of Poly(I:C)-injected dams exhibit behavioral deficits previously observed in this model (Choi et al., 2016; Estes and McAllister, 2016; Shin Yim et al., 2017; Kentner et al., 2019). We tested their offspring (male and female) in a battery of three behavioral assays (however, these initial cohort was not tested in the social touch assay). The MIA offspring were tested for the presence of ultrasonic vocalizations at P7-9, in the 3-chamber social interaction assay (which quantifies their preference to a novel mouse over an inanimate novel object) at P60-90, and in the marble burying assay (a measure of repetitive behaviors in rodents) also at P60-90 (Deacon, 2006; Yang et al., 2011; Choi et al., 2016; Shin Yim et al., 2017). PBS and MIA mice that were tested on the social touch behavioral assay were only characterized for IL-6 levels and did not undergo this battery of three behavioral assays.

Surgical implantation of head bars

Adult mice were anesthetized with isoflurane (5% induction, 1.5-2% maintenance via nose cone v/v) and secured on a stereotaxic frame (Kopf) via metal ear bars. A 1 cm long midline skin incision was made above the skull under sterile conditions. A titanium U-shaped head bar (3.15 mm wide x 10 mm long) was placed on the skull just caudal to Lambda and permanently glued with dental cement. This bar was later used to secure the animal to a post for the head-fixed social touch behavioral assay. This surgery lasted ~15-20 min and mice fully recovered within 30 min after surgery and returned to group-housed cages.

Social touch assay in head-restrained mice

Following head bar implantation, mice were habituated to head restraint and to running on an air-suspended 200 mm polystyrene ball, as well as to the movement of a motorized stage that was used for repeated presentations of an inanimate object or a stranger mouse. The stage was controlled through MATLAB (Mathworks) in a custom-built, sound-attenuated behavioral rig (93 cm x 93 cm x 57 cm) that was dimly illuminated by two infrared lights (Bosch, 850 nm) (**Fig. 1a**). For habituation, test mice were placed on the ball for 20 min each day for 7-9 consecutive days before testing. In parallel, 'visitor' mice (stranger to the test mouse) were habituated to head-restraint in a plexiglass tube (diameter: 4 cm) secured to a motorized stage consisting of an aluminum bread board (15 x 7.6 x 1 cm) attached to a translational motor (Zaber Technologies, X-LSM100A). The stage translated at a constant speed of 1.65 cm/s. The neutral starting position was 6 cm away from the test mouse.

Following habituation, test mice were subjected to both voluntary and forced interactions with a visitor mouse or a novel inanimate object (a plastic 50 mL Falcon conical centrifuge tube, Fisher Scientific) over the course of 2 d (**Fig. 1b**). Voluntary interactions meant that the test mouse was within whisker contact of the novel object or mouse, while in forced interactions the stage stopped at a position closer to the test mouse such that the tip of the object or snout of the visitor mouse was in direct contact with the snout of the test mouse (**Movies 1-3**). These positions were calibrated before each experiment. On day 1, test mice were placed on the ball and recorded for a 2 min baseline period (the plexiglass tube on the moving stage was empty). Next, we inserted the novel plastic object (50 mL Falcon tube) into the plexiglass tube on the motorized stage. For this control interaction the test mouse first experienced a 2 min period of no touch but was able to visualize the object in the neutral position (before touch, 6 cm away). Next, the motorized stage moved the object to within whisker reach of the test mouse for a total of 5 or 20 such presentations of voluntary object touch (**Movie 2**). Each bout lasted 5 s, with a 5 s interstimulus interval (ISI)

during which the platform moved away by 1 cm and the object was out of reach of the test mouse. The total travel time for the platform was 1.2 s (for back and forwards). After this voluntary object touch session, the test mouse was returned to its cage to rest for at least 60 min before being head-restrained again on the ball to undergo voluntary or forced social touch (randomized) session with a visitor mouse. A same-sex, same age (P60-90) novel WT mouse (for WT and *Fmr1* KO test mice) or a novel PBS mouse (for PBS and MIA test mice) was head-restrained inside the plexiglass tube on the stage. Following a 2 min period in the neutral position where the test mouse could see but not touch the stranger mouse, the motorized stage moved to the position for voluntary social touch (whisker-to-whisker) (**Movie 3**) or forced social touch (snout-to-snout) (**Movie 1**) for 5 or 20 bouts of each (also lasting 5 s with a 5 s ISI where the mouse on the platform moved out of reach of the test mouse). The test mouse was then returned to its cage for 24 h. On day #2, the mouse was placed back on the ball again for a 2 min baseline period followed by a 2 min period of no touch with a different stranger mouse. Depending on if the test mouse received voluntary or forced social touch on day 1, the mouse received 5 or 20 presentations of the alternate touch type with the second stranger mouse (**Fig. 1c**).

Additionally, we tested a separate cohort of WT and *Fmr1* KO mice on 20 presentations of forced touch from a novel plastic object (a 50 mL Falcon tube), a novel inanimate furry toy mouse (PennPlax) onto which we glued Nylon whiskers (1.5 cm length, 0.5 cm thickness), a stranger mouse of the opposite sex, and a familiar same-sex mouse. In this cohort, the test animal received forced object touch followed by forced social touch on the same day. On the next day, the animal received touch from an inanimate toy mouse and on day 3, the animal received touch from a stranger mouse of the opposite sex. Finally, the test mouse received voluntary social touch from stranger mouse on day 4. 24 hours later, the test mouse received forced social touch from the same mouse used on day 4 (now ‘familiar’, given the repeated exposure).

QUANTIFICATION AND STATISTICAL ANALYSES

Behavioral analyses

During the course of the assay, high-resolution videos (.mp4 or .avi files) were recorded of the test mouse's eye, face, and body with 3 cameras (either The Imaging Source, Monochrome USB3 or Teledyne Flir, Blackfly S USB3) at 50 FPS (Figs. 3-6) or 120 FPS (Figs. 7-8) for behavioral analyses. Avoidance running, aversive facial expressions, pupil diameter and locomotion were analyzed from these videos of the eye, face, and body (**Fig. 1d**). Running avoidance (backwards directed running), running speed and locomotion were analyzed from body videos using custom-written video analysis routines in MATLAB. Painted dots on the polystyrene ball (1 cm diameter) were used to measure the angle and distance based on the displacement of each dot at a frame to the closest dot 5 frames later (median angle and distance was calculated using all angles and distances for dots displaced for every 5 frames, or 0.1 s). Median angle was used to determine the direction the animal was moving toward, while distance was used to calculate running speed. All videos were visually inspected post-hoc to correct for values corresponding to grooming or other sudden movements (so that those would not be considered as directional running). Locomotion was characterized as whenever the animal was actively moving on the ball in the video. In a second cohort of *Fmr1* KO mice and WT controls, we used recorded videos at 120 FPS, and used a modified manual scoring of avoidance running because automated detection of three or more dots on the ball was not possible due to lighting conditions or fading of painted dots (He et al., 2017). Pupil diameter was quantified using *Facemap* (Stringer et al., 2019) and MATLAB. Aversive facial expressions (AFEs; i.e., prolonged whisker protraction and orbital tightening) were analyzed using *DeepLabCut* (Mathis et al., 2018; Nath et al., 2019). Briefly, the network was trained on images from the face videos to identify markers on the mouse's whisker follicles. The displacement of the follicles was calculated using these markers to detect sustained (≥2 s) negative displacements from the resting position of the whiskers as aversive whisker protraction movements. Analysis of the whisker displacement was semi-automated; all videos were inspected post-hoc to exclude frames when grooming and other movements

obscured the face or certain whisker movements interfered with the detection of sustained whisker protraction. We quantified overall active whisking during the assay by calculating the motion energy of whisking using *Facemap*. To quantify orbital tightening or eye squinting, a neural network was trained on still images from videos of the face to reliably identify markers along the mouse's eye. The area of the eye was calculated from these markers to quantify orbital tightening. For analysis of pupil diameter and orbital tightening, we excluded video frames when blinking, grooming, or other movements obscured the animal's face.

Because there are important sex differences in both the prevalence and symptoms of ASD (Werling and Geschwind, 2013; Bartholomay et al., 2019), we distinguished males from females across all figures (squares = males, circles = females).

Statistical analyses

Statistical tests were performed in Prism software (GraphPad). Statistical analyses of normality (Lilliefors and Shapiro Wilk tests) were performed on each data set; if data deviated from normality ($p<0.05$) or not ($p>0.05$), appropriate non-parametric and parametric tests were performed. For parametric two-group comparisons, a Student's t-test (paired or unpaired) was used. For non-parametric tests, we used Mann-Whitney test (two groups) and the Kruskall-Wallis test (repeated measures). Multiple comparisons across touch conditions and genotypes/groups were analyzed using two-way ANOVA with post-hoc Bonferroni's test. If data was non-normal, we applied a logarithmic transformation on the data and compared the two-way ANOVA with and without the transformation. Since the statistical output of the two-way ANOVA was similar for the transformed and the non-transformed, non-normal data, we used the statistical output from the latter. All experiments were conducted in at least two litters per genotype/group. Graphs either show data from each mouse per group or group means (averaged over different mice) superimposed on individual data points. In all figures, the error bars denote standard error of mean (s.e.m.).

Data and code availability

Code used in MATLAB for analysis of DeepLabCut and Facemap files and ball motion videos is available here: https://github.com/porteralab. Data will be made available upon request.

RESULTS

A novel behavioral assay for social touch

To investigate how mice respond to social touch, and the circuits involved, one must consider the pros and cons of different behavioral assays. Inspired by prior designs of social touch assays for mice and rats (Bobrov et al., 2014; Jennings et al., 2019; Resendez et al., 2020; Jeon et al., 2023), we designed a novel head-fixed behavioral assay in which we can control the frequency and duration of each social touch interaction, the type of touch (whisker-whisker vs. snout-snout), and the context (social vs. object). In this this assay, a head-restrained test mouse that is allowed to run on an air-suspended polystyrene ball is monitored with multiple cameras during repeated presentations of a novel mouse that is also head-fixed and resting on a motorized stage that brings it to predetermined positions at various distances away from the test mouse (see *Methods*, **Fig. 1a-c**). We tested three different positions of the stage to assess corresponding conditions of social touch: 1. Before touch, where the test animal can see the novel 'visitor' mouse but not touch it; 2. Voluntary social touch where the test mouse can interact with the visitor via its whiskers; 3. Forced social touch, where the visitor mouse is so close to the test mouse that their snouts are in direct physical contact.

By using high frame rate cameras to record the test animal's face and eyes, as well as ball motion, we can quantify different aspects of facial expressions (e.g., whisker movements, mouth opening, ear movements, eye size changes) and changes in pupil diameter or saccades, as well as locomotion (see Materials & Methods; **Fig. 1d**). Because we are interested in autism, we focused on behaviors that might indicate that the mouse experienced social touch as an

unwanted aversive stimulus, by exhibiting avoidance, defensive behaviors, facial expressions of negative emotion, or hyperarousal. Indeed, these behavioral responses are observed in ASD individuals responding to social or affective touch and in mouse models of ASD responding to passive non-social touch (Cascio et al., 2008; Klusek et al., 2013; Mammen et al., 2015; He et al., 2017; Bales et al., 2018; Thye et al., 2018; Zampella et al., 2020). Our assay also examines social touch that is potentially unpleasant, rather than allo-grooming, by including forced snout-snout interactions. This allowed us to explore how ASD mouse models might respond to social touch across different contexts and how the tactile system engages with these stimuli behaviorally. However, this assay can be easily modified to change the presentation parameters, or the types of visitor and test mice (e.g., age, sex, genotype), in order to explore a myriad of interesting questions about social touch in rodents. We also designed the assay to be compatible with calcium imaging or silicon probe recordings of neural activity, to elucidate circuits that are activated by social touch, as well as those that mediate behavioral responses to social touch.

To demonstrate the utility of this novel social touch assay, we compared the behavioral responses of control wild-type (WT) mice to those of two mouse models of ASD. The first was the *Fmr1* knockout (*Fmr1* KO) mouse model of Fragile X Syndrome (FXS) (The Dutch-Belgian Fragile X Consortium, 1994), the leading single gene cause of intellectual disability and autism. The other was the Poly(I:C) maternal immune activation (MIA) model, which is widely used as a model of an environmental cause of autism (Choi et al., 2016; Estes and McAllister, 2016; Kentner et al., 2019). Of note, we characterized the MIA model both as far as IL-6 levels in the dam and various behavioral deficits in the offspring (**Fig. 2**). We found that MIA mice exhibited reduced pup USV calls, reduced social preference, and increased marble burying compared to offspring of PBS-injected dams (**Fig. 2b**; marble burying: $p=0.0104$; USVs: $p=0.0435$; 3-chamber: $p < 0.0001$).

Below, we present results of our observations related to four major behavioral responses: 1. Avoidance running; 2. Pupil dilation; 3. Whisker protraction; and 4. Orbital tightening (squinting).

Overall, we hypothesized that, compared to their respective controls, *Fmr1* KO and MIA mice would show increased avoidance, hyperarousal, and more AFEs (whisker protraction, eye squinting) to social touch that controls, but no differences for object touch. Furthermore, we expected that forced social touch (snout-snout) would be more aversive than voluntary social interactions (whisker-whisker) for ASD mice.

Greater avoidance running in Fmr1 KO and MIA mice during social touch but not object touch

Sensory hypersensitivity is very prevalent in ASD and is thought to contribute to maladaptive avoidance responses, such as tactile defensiveness and social avoidance (Baranek et al., 1997; Robertson and Baron-Cohen, 2017). Most children with FXS experience sensory over-reactivity, often leading to tactile defensiveness and gaze aversion (Sinclair et al., 2017; Rais et al., 2018). However, avoidance to social touch per se has never been investigated in animal models of ASD or FXS. Previously, we demonstrated that *Fmr1* KO mice exhibit tactile defensiveness to repetitive whisker stimulation, which manifested as avoidance running (He et al., 2017). To investigate whether social touch leads to avoidance, we quantified running direction of the test mouse relative to the novel object or stranger mouse (**Fig. 3a**). If the test animal was moving backward (either left or right), we categorized this as avoidance, in contrast to running forward, which was considered an adaptive response (seeking social interaction). We initially calculated the total time the mouse spent in locomotion, regardless of direction, to determine if group differences in running might skew the proportion of avoidance running. Although there are reports of hyperactivity in *Fmr1* KO mice (The Dutch-Belgian Fragile X Consortium, 1994; Sullivan et al., 2006), we have not found differences in total locomotion between adult *Fmr1* KO and WT mice either in response to whisker stimulation or while performing a visual discrimination task (He et al., 2017; Goel et al., 2018). In the social touch assay, we observed that mice of all groups spent more time running when they transitioned from the baseline period (before touch) to the period of social touch ($p<0.05$), but there were no significant group differences ($p>0.05$ between

WT vs *Fmr1* KO & PBS vs MIA, **Table 1**). There were also no differences in running speed during object or social touch between *Fmr1 KO* or MIA mice and their respective controls (**Fig. 3b**).

In contrast, when we compared the proportion of time that mice spent showing avoidance running as a proportion of total locomotion, we found that both *Fmr1* KO and MIA mice displayed higher avoidance during voluntary and forced social touch compared to controls, but not during voluntary object touch (**Fig. 3c**; WT vs. *Fmr1* KO: vol. object $p>0.05$, vol. social $p=0.006$, forc. social $p=0.047$; PBS vs. MIA: vol. object $p>0.05$, vol. social $p=0.002$, forc. social $p=0.002$). Thus, considering overall running speed was similar between the two ASD models and their controls both before and during social touch, these differences in avoidance running could not be explained by hyperactivity.

Because there are important sex differences in both the prevalence and symptoms of ASD (Werling and Geschwind, 2013; Bartholomay et al., 2019), we also compared avoidance between male and female mice in each group, but did not find any significant sex differences within genotype. We also looked at differences between litters in each genotype but did not see any obvious differences either, although the sample size per litter was small (2-9 mice per litter, median = 5 mice).

Pupil dilation with social touch lasts longer in Fmr1 KO, but not MIA mice

Autonomic hyperarousal, including elevated heart rate and pupil dilation, is observed in autistic individuals during tactile stimulation or affective touch, and is used as an indicator of tactile hypersensitivity (Heilman et al., 2011; McGlone et al., 2014; Fukuyama et al., 2017). We measured changes in pupil size as a proxy for arousal in response to social touch (**Fig. 4a, Movie 4**). We first compared pupil size as a mean of the first 5 presentations and found no differences between WT and *Fmr1* KO or between PBS and MIA mice, regardless of condition (object or social touch). Next, because pupils can dilate or constrict over short time scales, we compared pupil size at individual presentations of object or social touch (Vinck et al., 2015; Joshi and Gold,

2020). We found that, in all groups, pupils significantly dilated to a similar extent after the first object/mouse presentation (**Fig. 4b)**. Interestingly, after repeated presentations of voluntary object touch, pupil size returned to baseline in all groups, presumably as a form of adaptation to a non-threatening situation (**Fig. 4b**). In contrast, pupils remained dilated for a longer period in *Fmr1* KO mice with both voluntary social touch and forced social touch whereas they constricted to baseline in MIA mice and controls. The difference was most pronounced with forced social touch, where pupils were significantly larger in *Fmr1* KO mice than in their controls on the 5th presentation (**Fig. 4b**; pupil size: WT vs. *Fmr1* KO $p<0.001$, PBS vs. MIA $p>0.05$).

In a subset of these mice that we tested up to 20 presentations of forced social touch, we found that pupil size in *Fmr1* KO and MIA mice eventually returned to baseline (**Fig. 4c**). We did not find any sex or litter differences in pupil size before or after social touch. Altogether, these findings indicate that *Fmr1* KO mice display more hyperarousal than WT mice to social touch.

Aversive facial expressions (grimace) are more pronounced in Fmr1 KO and MIA mice during forced social touch

In humans, facial expressions are considered good indicators of emotional state (Anderson and Adolphs, 2014). Autistic individuals will grimace or wince to aversive sensory stimuli and will avert their gaze during social interactions (Kliemann et al., 2010; Foss-Feig et al., 2012; Schmitt et al., 2014). Facial grimacing in the form of orbital tightening, changes in whiskers, or nose bulging, is also observed in rodents experiencing pain (Langford et al., 2010), but less is known about which facial expressions are associated with sensory hypersensitivity or unwanted social interactions. We posited that if ASD mice consider social touch as aversive, they would manifest facial grimacing. We focused on two facial features, whisker movement and orbital tightening (**Movie 5**), because they were easily detectable by cameras in our set-up and because analysis could be semi-automated using *DeepLabCut* (Langford et al., 2010; Mathis et al., 2018). For whisker movement, we quantified bouts of sustained whisker protraction (**Movie 5**), which is

often seen in mice experiencing pain (Langford et al., 2010), in mice during active escape, and during aggression or immediate facial contact (Wolfe et al., 2011; Defensor et al., 2012; Dolensek et al., 2020; Ebbesen and Froemke, 2021). Prolonged whisker protraction is different from active whisking, which is an adaptive behavior in rodents as they explore their environment, both in terms of the speed and the direction of whisker movement. During active whisking, follicles are displaced forwards and backwards rapidly and rhythmically (8-12 Hz, for bouts lasting 1-2 seconds) (Bush et al., 2016). In contrast, during aversive whisker protraction, the animal's whiskers are maintained in a fixed, forward position for bouts lasting up to several seconds.

We could distinguish between these two types of whisker movement using *DeepLabCut* and *Facemap* (**Fig. 5a**; see Methods). ASD mice and their controls showed more active whisking when presented with novel mice compared to before touch (**Fig. 5b,** $p<0.05$), but we did not find any significant differences in time spent actively whisking between groups or between voluntary or forced social touch. However, we found that *Fmr1* KO and MIA mice spent significantly more time than their controls displaying aversive whisker protraction during forced social touch (**Fig. 5c**, WT vs. *Fmr1* KO $p=0.013$, PBS vs. MIA $p=0.034$). In contrast, we saw no group differences in whisker protraction during object touch or voluntary social touch. There were also no significant sex or litter differences in whisker protraction in any group across all touch conditions.

Next, we determined whether mice show orbital tightening during social touch by estimating the area of the eye during the first 5 presentations of social touch. Again, we used *DeepLabCut* to train a neuronal network to estimate the area of the eye (**Fig. 6a)**. We found that orbital area (relative to the period before touch) was significantly smaller (i.e., more orbital tightening) in *Fmr1* KO mice, and to a lesser extent in MIA mice, during forced social touch, but not during voluntary object or voluntary social touch, and not at all in the WT or PBS controls (**Fig. 6b**, WT vs. *Fmr1* KO $p=0.0065$, PBS vs. MIA $p=0.051$). The total area of the eye (in pixels) was also significantly smaller in *Fmr1* KO mice than in WT controls during forced social touch compared to just before touch (**Fig. 6c**, WT $p>0.05$ vs. *Fmr1* KO $p=0.0021$). In contrast, when we

quantified the eye area before and during voluntary social touch, we found no significant differences in *Fmr1* KO mice (**Fig. 6c**, $p>0.05$). In the MIA mice, there was a slight decrease in the area of the eye during forced social touch, but this did not reach significance ($p=0.091$). Interestingly, some control mice, especially the PBS controls, tended to open their eyes more during social touch (**Fig. 6c**, PBS $p=0.047$; WT $p<0.05$), which could represent increased arousal towards the other mouse. These findings suggest that AFEs like sustained whisker protraction and forceful eye closure are uniquely triggered by forced social interactions in ASD mouse models, particularly in the FXS model.

Fmr1 KO *mice show greater avoidance and AFEs during forced interactions with stranger mice than WT controls (but similar maladaptive responses to forced object touch)*

After completing this initial set of experiments, we considered the possibility that direct, forced contact with an inanimate object (particularly if it resembled a mouse) might elicit as much avoidance, hyperarousal, and increased AFEs in ASD mice as forced contact with a mouse (i.e., forced social touch). Indeed, people with ASD also exhibit tactile defensiveness to certain textures (He et al., 2017; Green et al., 2018). Because *Fmr1* KO mice had shown the largest differences with the social touch assay, we focused on this model for these additional control studies.

In an initial set of experiments, we tested how a new cohort of WT and *Fmr1* KO mice ($n=12$ and 10, respectively) responded to forced contact with the same novel object, a plastic 50 mL tube. In WT animals, forced touch with this object led to significantly greater running avoidance and whisker protraction than forced social touch, suggesting that social contact is better tolerated in WT animals (**Fig. 7b**, WT social vs. object, $p<0.001$ for avoidance and $p=0.009$ for whisker protraction). In contrast, in *Fmr1* KO mice, the difference between forced object touch and forced social touch was much smaller and did not reach significance for whisker protraction (**Fig. 7b**, *Fmr1* KO social vs. object, $p=0.025$, $p>0.05$, respectively). As a result, we found higher avoidance and whisker protraction in *Fmr1* KO compared to WT controls for forced social touch, but not for

forced object touch (*Fmr1* KO vs. WT, p=0.079 for avoidance, p=0.031 for whisker protraction). Furthermore, we observed a slightly smaller orbital area in *Fmr1* KO mice than in WT controls during the last 5 presentations of forced social touch, but not with forced object touch (**Fig. 7b**, WT vs. *Fmr1* KO social p=0.232, object p=0.382). Note that orbital tightening in this new cohort of *Fmr1* KO mice was more prominent in the last 5 presentations, whereas it was present after only 5 presentations (and persisted) in the original cohort (**Fig. 6**). This likely reflects the smaller sample size and/or differences in behavioral habituation across batches of *Fmr1* KO mice (He et al., 2017).

Because the plastic tube is smooth, it may not be as aversive as the whiskers and fur of another mouse. Therefore, in a second set of control experiments with the same cohort of WT and *Fmr1* KO mice, we tested forced object touch using an inanimate plush toy mouse with fur and whiskers. Strikingly, we found that WT and *Fmr1* KO mice reacted very similarly to forced touch from the toy mouse as they did to the plastic tube, with greater avoidance and aversive whisking in WT mice to this object than to a forced social interaction with a stranger mouse (**Fig. 7c**, WT social vs. object, p=0.029 for running avoidance, p=0.001 for whisker protraction). Once again, *Fmr1* KO mice showed similar degrees of avoidance and whisker protraction to forced object and social touch (*Fmr1* KO social vs. object p>0.05 for both), but significantly more orbital tightening than WT mice to only forced social interactions (*Fmr1* KO vs. WT, p=0.031). Incidentally, when we compared the behavioral responses of WT and *Fmr1* KO mice to forced presentations of the 50 mL tube and the plush toy, we did not find significant differences in AFEs between these two objects (p=0.0674-0.999 for WT and p=0.395-0.415 for *Fmr1* KO), although *Fmr1* KO mice had slightly less running avoidance to the plush toy (p=0.029). Together, these results suggest that whereas forced touch from any object (smooth plastic tube or furry toy mouse) elicits similar maladaptive behaviors in WT and *Fmr1* KO mice, *Fmr1* KO mice are uniquely sensitive to forced social interactions with another live mouse.

Fmr1 KO mice show less aversion to social touch with a mouse of the opposite sex, but whether the other mouse is familiar or a stranger matters less

Another important control related to social touch was to determine whether the sex of the visitor mouse influenced the degree of aversion it might elicit in ASD mice. For example, it is well-established that sensory inputs from mice of the same sex triggers aggression in males, whereas interactions with opposite sex animals leads to mating responses (Chen and Hong, 2018). Furthermore, female mice generally show more preference to males, though this tends to depend on receptivity (Chen and Hong, 2018). Therefore, we sought to determine if the maladaptive behavioral responses to forced social touch are just as pronounced with a stranger mouse of the opposite sex (**Fig. 8a**). In general, WT mice showed similarly low levels of avoidance and AFEs when interacting with mice of either sex (**Fig. 8b**, $p>0.05$). In contrast, *Fmr1* KO mice showed more running avoidance and aversive whisking with a stranger mouse of the same sex than with opposite sex mice (**Fig. 8b**, $p=0.067$ for avoidance and $p=0.0213$ for whisker protraction). The magnitude of avoidance to stranger mice (this time of the opposite-sex) was significantly higher in *Fmr1* KO mice than in WT mice, further supporting our previous observations regarding social touch with same sex mice (**Fig. 8b**, WT vs. *Fmr1* KO $p=0.0374$). *Fmr1* KO mice also showed significantly more orbital tightening than WT controls during forced social interactions with mice of the same sex, but not with mice of the opposite sex ($p=0.035$ and $p>0.05$, respectively).

We next tested if aversion to forced social touch in *Fmr1* KO mice depended on whether the other mouse was familiar or a stranger. Some autistic individuals have difficulty recognizing and recalling faces of strangers (Williams et al., 2005; Stantić et al., 2022). Similarly, the Shank3B model of ASD shows deficits in discriminating between a novel and a familiar mouse (Cope et al., 2023). In our social touch assay, we observed that *Fmr1* KO mice (n=8-10) exhibit similar levels of aversion to forced social touch with a familiar mouse and a stranger mouse (same-sex) (**Fig. 8c**, $p>0.05$ for avoidance and AFEs). Further confirming our previous results, this new cohort of *Fmr1* KO mice again showed significantly greater avoidance and a trend toward greater whisker

protraction to forced social touch with a familiar mouse than did WT mice (n=11-12) (**Fig. 8c**, $p<0.001$ and $p=0.141$, respectively). Interestingly, WT mice showed a smaller orbital area during forced social touch with a familiar mouse relative to a stranger mouse (**Fig. 8c**, $p=0.011$). We surmised that repetitive presentations of social touch with the same animal over 2 d may elicit some anxiety in WT animals. Overall, these control experiments confirm that *Fmr1* KO mice show significantly more maladaptive responses to social touch than WT mice, and more avoidance/AFEs to opposite-sex mice than same-sex mice, but that it matters much less whether mice are familiar or stranger to them.

DISCUSSION

The main goal of this study was to implement a new behavioral paradigm that could be used to investigate social touch behaviors in rodents and the underlying circuits involved. Our findings can be summarized as follows: 1. Our new social touch assay can reliably distinguish behavioral responses of mice to social touch from their responses to object touch; 2. Relative to typically developing control mice, both *Fmr1* KO and MIA mice show increased avoidance running to both voluntary and forced social touch, but not to voluntary object touch; 3. Hyperarousal (as measured by pupil dilation) to social touch lasts longer in *Fmr1* KO mice but not MIA mice compared to their controls; 4. AFEs to social touch are more pronounced in ASD mice than in controls, especially during forced social touch; 5. *Fmr1* KO mice show similar aversion to forced object touch as WT controls but significantly greater aversion to forced social touch; and 6. Social touch from same-sex mice elicits greater avoidance and AFEs in *Fmr1* KO ASD mice, but whether the other mouse is familiar or a stranger does not matter.

A few prior studies had investigated social touch in freely moving rodents (Bobrov et al., 2014; Jennings et al., 2019; Yu et al., 2022). Despite their ingenuity, the assays relied on at least one animal initiating social touch, and they could not focus on any particular aspect of social touch (e.g., face-to-face contact) amongst the broad and complex behavioral repertoire (e.g., ano-

genital sniffing, allo-grooming). Moreover, while naturalistic in their design, those assays were limited by the fact that individual social touch interactions varied in duration and frequency. We purposely designed a new assay for head-fixed rodents so the experimenter could control all aspects of the social touch interaction, from the duration and number of interactions to the context of the interaction (voluntary vs. forced, object vs. social). This allowed us to monitor various behavioral responses of the animal to social touch, including body movements that indicated avoidance, facial expressions suggestive of aversion, and dilated pupils reflecting hyperarousal/anxiety. Importantly, our assay could easily be combined with 2-photon calcium imaging and/or silicon probes to record neural activity during social interactions. Because the social touch presentations are highly stereotyped across large numbers of trials, the data from neural recordings would be highly reproducible, and one could quantify the degree to which neurons adapt their responses to repeated presentations. Thus, our assay should be of help to neuroscientists interested in investigating social behaviors in rodents and the circuits involved.

To validate this assay, we probed social touch within a disease context in which social deficits are observed, by examining two different mouse models of ASD. A major gap in our understanding of ASD, particularly when using mouse models, concerns the relationship between tactile hypersensitivity and social deficits (Suvilehto et al., 2015; Thye et al., 2018; Lee Masson et al., 2019). Therefore, we used our social touch assay to characterize three maladaptive behavioral responses to social touch in well-established mouse models of ASD: avoidance running, hyperarousal, and AFEs.

We previously reported avoidance and defensive gestures to repetitive whisker stimulation in *Fmr1 KO* mice (He et al., 2017; Kourdougli et al., 2023). However, avoidance to social touch was not simply a manifestation of generalized sensory hypersensitivity (tactile defensiveness) because it occurred in the context of social touch and not voluntary object touch (**Fig. 3c**). Similar sensory avoidance is also observed in humans with ASD and FXS (Green and Ben-Sasson, 2010; Mammen et al., 2015; Rais et al., 2018). Escape or avoidance has been described in mice

responding to threatening stimuli, or those causing discomfort, anxiety or pain (Yilmaz and Meister, 2013; Gehrlach et al., 2019; Huang et al., 2019; La-Vu et al., 2020). It will be important to determine whether other avoidance behaviors, such as defensive grooming or gaze avoidance, can also be detected using our social touch assay (Kleberg et al., 2017; Stuart et al., 2022).

The maladaptive behaviors to social touch were not the same in both ASD models. For example, orbital tightening to forced social touch were more prominent in *Fmr1* KO mice than in the MIA model (**Fig. 6b,c**), and only the *Fmr1* KO model exhibited sustained pupil dilation, particularly for forced social touch (**Fig. 4b,c**). Pupil size is commonly used as an indicator of arousal levels and autistic/FXS individuals show deficits in autonomic regulation, including hyper- and hypo- arousal (Klusek et al., 2013; Kushki et al., 2014; Vinck et al., 2015; Cuve et al., 2018; Joshi and Gold, 2020). Interestingly, some autistic individuals who do not exhibit hyperarousal fail to show sensory hypersensitivity (Rogers and Ozonoff, 2005), suggesting that the two phenomena may be strongly correlated. However, aside from pupil size, hyperarousal can manifest with other autonomic responses, such as changes in heart rate, perspiration, or breathing (Heilman et al., 2011; Kushki et al., 2014), which could also be monitored during social interactions with our assay.

The observation that ASD mice exhibit more pronounced AFEs during forced social touch aligns well with previous findings concerning facial grimacing in mice (Langford et al., 2010; Defensor et al., 2012; Dolensek et al., 2020; Ebbesen and Froemke, 2021). Since the Mouse Grimace Scale (MGS) has been widely adopted to quantify responses to pain, it could also be combined with our assay. Autistic people are often unable to recognize or imitate facial expressions of others, which complicates their interactions in social settings (Drimalla et al., 2021). We did not monitor the facial expressions of the stranger/familiar mice, but the camera setup could be modified to track this too.

Given that forced social touch elicited more pronounced behavioral deficits than voluntary social touch in ASD mice, it was critical to compare responses of *Fmr1* KO mice to forced social

touch and forced object touch. Although both a Falcon tube and an inanimate toy mouse (similar shape and texture as a mouse) resulted in similar levels of avoidance and AFEs between WT and *Fmr1* KO mice, we repeatedly found that forced social interactions were only deemed aversive by the latter. A previous study found that social interaction was more preferable to WT mice than object interaction (Yang et al., 2011). Thus, while forced interactions with any object are aversive to WT and *Fmr1* KO mice, only WT animals find forced social interactions more tolerable. Viewed differently, *Fmr1* KO mice exhibit a general hypersensitivity to all tactile stimuli, but they fail to down-modulate this aversion in the context of social interactions the way WT controls can. This unique deficit in the social context of *Fmr1* KO mice deserves further investigation.

In general, mice tend to prefer social interactions with mice of the opposite sex (Chen and Hong, 2018). Opposite-sex social interactions have not been studied extensively in ASD models, although one study found that 16p11.2 deletion mice exhibit fewer vocalizations in the presence of mice of the opposite sex (Yang et al., 2015). We observed that *Fmr1* KO mice show milder impairments (less avoidance and no AFEs) during opposite-sex interactions (**Fig. 8b**). This would suggest that, even though ASD mice show maladaptive responses to opposite sex interactions relative to WT animals, they prefer it to same-sex interactions.

Finally, we observed ASD mice display similar levels of avoidance and AFEs in response to forced social touch from a familiar mouse relative to a stranger mouse. This finding was not unusual given that both ASD individuals and mouse models display deficits in social memory (Williams et al., 2005; Stantić et al., 2022; Cope et al., 2023).

We did not find significant sex differences in our assay. This was surprising given that the prevalence of ASD and the range of phenotypic behaviors are different in males and females (Werling and Geschwind, 2013). It is possible that sex differences were not apparent in our head-fixed social touch paradigm because our sample size was not large enough, or because mice could not freely choose to engage in social investigation. However, our assay could easily be modified to allow the test mouse to exert control of the motorized stage.

We recognize that our social touch assay has some limitations. Compared to assays for freely moving mice, our assay is less naturalistic. In spontaneous social interactions, mice are free to decide when to approach another animal. They may choose to approach other mice from the rear, as opposed to face-to-face. Our head-fixed assay also prevents the mice from engaging in other socially relevant behaviors that involve touch, such as allo-grooming, or fighting. Head-fixation also prevents head movements that may be important for mice to engage in social touch.

In summary, our novel head-fixed paradigm revealed that ASD mouse models manifest a shared repertoire of maladaptive responses to social touch and that these behavioral manifestations align well with symptoms and atypical behaviors observed in autistic humans. The fact that two rather distinct ASD models exhibited very similar behavioral phenotypes in avoidance, arousal and facial expressions suggests that our assay may uncover remarkable phenotypic convergence in social touch deficits in other ASD models (despite differences in arousal). Future studies could also explore social touch in other contexts, such as mother-to-pup interactions, or age dependent differences. Finally, one could utilize this assay in combination with in vivo 2-photon calcium imaging or silicon probes to explore changes in neural activity in relevant brain circuits in mouse models of neurodevelopmental conditions.

FIGURE LEGENDS

Table 1: Locomotion increases when mice engage in object or social touch and does not differ between mouse models of autism and their controls

Fig. 1: Setup for social touch behavioral assay

a. Overview of head-fixed setup for the social touch behavioral assay. A head-fixed test mouse can run on an air-suspended polystyrene ball while interacting with a stranger mouse restrained in a plexiglass tube secured to a motorized platform. The system is fully automated to move the stranger mouse to different distances away from the test mouse. Two cameras focus on the face and the eye/pupil, respectively, while a third camera that tracks the mouse and ball motion is overhead (not shown). An infrared light source provides optimal light for tracking behavioral responses. Acoustic foam is used for sound insulation.

b. We tested three types of touch: voluntary object (whisker-object), voluntary social (whisker-whisker), and forced social (snout-snout).

c. Duration of baseline (platform empty without object/mouse), no touch, and object social touch, as well as the number of stimulations and delay between each type of touch condition.

d. Camera views for tracking ball motion, pupil size and AFEs.

Fig. 2: Interleukin-6 levels are higher in pregnant dams injected with Poly(I:C) and their offspring show expected behavioral deficits

a. MIA was induced in pregnant dams by intraperitoneally injecting Poly(I:C) at embryonic age 12.5 (E12.5). Interleukin-6 (IL-6) cytokine levels are higher in pregnant dams injected with Poly(I:C) at E12.5 compared to dams injected with PBS. Two different Poly(I:C) lots acquired from Sigma-Aldrich were tested and elicited significantly higher IL-6 levels in dams. $^{**}p<0.01$, $^{*}p<0.05$ for Mann-Whitney test.

b. Offspring of dams injected with Poly(I:C) from Lot A and B showed increased fraction of marbles buried in the marble burying assay at P60-90, reduced ultrasonic vocalizations recorded at P7-9, and no difference in preference for a novel mouse versus novel object in the 3-chamber social interaction assay. Squares = males, circles = females in panel b. ***p<0.001, *p<0.05, unpaired t-test for marble burying assay and USVs, two-way ANOVA with Bonferroni's for 3-chamber social assay.

c. IL-6 levels in PBS and Poly(I:C) injected pregnant dams whose offspring were used for the behavioral testing in the social touch assay. Poly(I:C) from Lot A and B were used in pregnant dams.

Fig. 3: Mouse models of autism show avoidance to social touch from a stranger mouse

a. Analysis of locomotion and running speed and direction. Speed (cm/s) is calculated using the distance moved of a circle at time *t* to the closest circle in pixel space in time *t+5* every 5 frames (0.1 s). Direction of circle movement at time *t* to *t+5* frames is calculated from the angle between the circle at time *t* as the origin point relative closest circle at *t+5* in pixel space. Median speed and angle is calculated from distance and angle displacements of all circles every 5 frames (0.1 s). Locomotion is calculated by finding running speeds within 2 standard deviations of the mean speed. Example circle (red filled in time *t* and pink filled in *t+5*) moves to the right and up (red filled in time *t+5*, leftwards avoidance). Circles above red line are excluded from detection. Videos were inspected post-hoc to exclude frames when the animal was grooming or engaged in non-directed ball movements.

b. Average running speeds during all types of touch do not differ between ASD mice and control animals.

c. Running avoidance (backwards to left or right) is higher in *Fmr1 KO* and Poly(I:C) MIA mice compared to controls during voluntary and forced social touch but not object touch.

Squares=males, circles females. **p<0.01, *p<0.05, two-way ANOVA with Bonferroni's. No outliers were detected with ROUT's analysis.

Fig. 4: Pupil dilation is prolonged during social touch in ASD mice

a. Summary of pupil size analysis using Facemap. A region of interest (ROI) is drawn in the Facemap graphical user interface in Python (red circle). Facemap detects the pupil within the ROI (red dashed circle) and generates pupil area in pixels, which is converted to z-score in MATLAB.
b. Pupil size does not decrease to baseline levels (before touch) in *Fmr1 KO*, but does in MIA mice and both controls, by the 5th stimulation of voluntary and forced social touch. ***p<0.001, ** p<0.01, *p<0.05, two-way ANOVA with Bonferroni's for pupil area before touch vs. 1st and 5th stimulation.
c. A subset of mice were tested for up to 20 presentations of forced social touch. *Fmr1* KO mice, but not MIA mice, show persistent pupil dilation compared to their controls. Squares = males, circles = females. ***p< 0.001, **p<0.01, *p<0.05, two-way ANOVA with Bonferroni's before touch vs. each stimulation. No outliers were detected with ROUT's analysis.

Fig. 5: Prolonged whisker protraction during forced social touch in ASD mice

a. Summary of analysis for calculating prolonged whisker protraction and active whisking. To quantify periods of active whisking, we used Facemap. We denoted the whisker pad as a region of interest (ROI) and tracked changes in pixel value within the ROI as the motion energy for whisking. We then used MATLAB's findpeaks function to identify peaks and their local minima in the motion energy signal. We identified periods of active whisking as timepoints that were between the local minima of a peak. Whisking protraction was determined by training a deep neural network (NN) in DeepLabCut to detect 6 whisker follicles from a set of training video frames (randomly chosen frames). After training the NN and evaluating its performance, we processed full videos, which generated the x position of each whisker follicle in pixel space. We then

calculated the median change from all follicle positions relative to its resting position along the x-axis. Negative changes in follicle position at a given frame that were 1 standard deviation below mean resting position and lasted at least 2 seconds were denoted as periods of aversive whisker protraction.

b. Active whisking did not differ between *Fmr1* KO and MIA mice and their controls both before and during object and social touch. There was, however, a significant increase in mean whisking during the first 5 stimulations compared to before touch. Squares = males, circles = females. *p<0.05, **p<0.01 for two-way ANOVA with Bonferroni's. Vol = voluntary.

c. The fraction of time *Fmr1 KO* and MIA mice exhibited prolonged whisker protraction was higher during forced social touch than their controls but not significantly for voluntary object and social touch. Squares=males, circles=females. ***p<0.001 for two-way ANOVA with Bonferroni's. No mice were excluded according to ROUT's analysis.

Fig. 6: Orbital tightening during forced social touch in ASD mice

a. Summary of analysis for calculating orbital tightening. Orbital tightening is determined by training a deep neural network (NN) in DeepLabCut to detect 6 points along the eye from a set of training images (frames randomly chosen from videos). After training the NN and evaluating its performance, we inputed videos into the Deep NN, which outputs the XY position of each point on the eye in pixel space. We then used MATLAB to generate a polygon connecting the six dots and calculated the area of that polygon as the orbital area. Orbital area in pixels was normalized to the orbital area before touch.

b. Orbital area during touch is normalized to area before touch (object or mouse visible but no touch in behavior rig). Orbital area is significantly lower (greater orbital tightening) during forced social touch in *Fmr1 KO* and MIA mice (p=0.051) compared to controls. 1 WT, 2 *Fmr1* KO & 1 MIA mice detected as outliers with ROUT's analysis in panel b were also excluded from analysis in panel c.

c. Orbital area is significantly smaller during forced social touch compared to the period before touch in *Fmr1 KO* mice, but not in MIA mice (there is also a slight but significant increase in orbital area in PBS controls during forced social touch). Orbital area is not significantly changed during voluntary social touch. Squares=males, circles=females. ***p<0.001, **p<0.01, *p<0.05, two-way ANOVA with Bonferroni's.

Fig. 7: *Fmr1* KO mice show greater avoidance and AFEs than WT controls during forced social interactions (but similar maladaptive responses to object touch)

a. Summary of the different types of object touch (50 mL conical tube and plush toy mouse) and social touch interactions and experimental timeline for control experiments.

b. Running avoidance, fraction of time spent showing whisker protraction and orbital area for WT and *Fmr1* KO in response to forced social touch with a stranger mouse vs. forced object touch with 50 mL conical tube. ***p<0.001, **p<0.01, *p<0.05, two-way ANOVA with Bonferroni's.

c. Same metrics as in panel *b* but using an inanimate toy mouse as the object. **p<0.01,*p<0.05, two-way ANOVA with Bonferroni's.

Fig. 8: *Fmr1* KO mice show less aversion to social touch with a mouse of the opposite sex (but whether the other mouse is familiar or a stranger does not matter)

a. Summary of the different types of social touch (same vs. opposite sex; stranger vs. familiar) and experimental timeline for forced social touch.

b. Running avoidance, fraction of time spent showing whisker protraction and orbital area for WT and *Fmr1* KO in response to forced social touch with same-sex stranger vs. opposite-sex stranger. **p<0.01, *p<0.05, two-way ANOVA with Bonferroni's.

c. Same metrics as in panel *b* but using stranger vs. familiar mouse (always same sex). ***p<0.001, **p<0.01, *p<0.05, two-way ANOVA with Bonferroni's.

MOVIES

Movie 1: Five presentations of forced social touch

Representative video of forced social touch session. The movie shows the first 5 presentations of social touch with a stranger mouse. The platform is initially at 6 cm away, such that the stranger mouse is visible to the test mouse, but no touch is occurring. The platform then moves to a position where the two mice make direct snout-to-snout contact for 5 s then moves 10 mm away and stops beyond reach of their whiskers, and then moves back to the position for snout-to-snout contact.

Movie 2: A single presentation of voluntary object touch

Representative video of voluntary object touch session that displays the first presentation of a novel object (a plastic Falcon tube). The platform is initially at 6 cm away, such that the object is visible but no touch is occurring. The platform then moves to a position where the test mouse can make whisker contact with the object for 5 s.

Movie 3: A single presentation of voluntary social touch

Representative video of a voluntary social touch session that displays the first presentation of a stranger mouse. The platform is initially at 6 cm away, such that the stranger mouse is visible but no touch is occurring. The platform then moves to a position where both mice can voluntarily initiate whisker-to-whisker contact for 5 s.

Movie 4: Pupil dilation in mouse during social touch

Representative video of a forced social touch session from the camera view of the eye showing the pupil dilation upon social touch contact.

Movie 5: Aversive facial expressions in mouse during social touch

Representative video of a forced social touch session from the camera view of the face that demonstrate two different AFEs: 1. orbital tightening, and 2. switch from active whisking to aversive whisker protraction.

REFERENCES

Adolphs R (2009) The social brain: neural basis of social knowledge. Annu Rev Psychol 60:693-716.

Anderson DJ, Adolphs R (2014) A framework for studying emotions across species. Cell 157:187-200.

Bales KL, Witczak LR, Simmons TC, Savidge LE, Rothwell ES, Rogers FD, Manning RA, Heise MJ, Englund M, Arias Del Razo R (2018) Social touch during development: Long-term effects on brain and behavior. Neurosci Biobehav Rev 95:202-219.

Baranek GT, Foster LG, Berkson G (1997) Tactile defensiveness and stereotyped behaviors. Am J Occup Ther 51:91-95.

Baron-Cohen S, Belmonte MK (2005) Autism: a window onto the development of the social and the analytic brain. Annu Rev Neurosci 28:109-126.

Bartholomay KL, Lee CH, Bruno JL, Lightbody AA, Reiss AL (2019) Closing the Gender Gap in Fragile X Syndrome: Review on Females with FXS and Preliminary Research Findings. Brain Sci 9.

Bobrov E, Wolfe J, Rao RP, Brecht M (2014) The representation of social facial touch in rat barrel cortex. Curr Biol 24:109-115.

Bush NE, Solla SA, Hartmann MJ (2016) Whisking mechanics and active sensing. Curr Opin Neurobiol 40:178-188.

Cascio C, McGlone F, Folger S, Tannan V, Baranek G, Pelphrey KA, Essick G (2008) Tactile perception in adults with autism: a multidimensional psychophysical study. J Autism Dev Disord 38:127-137.

Chen P, Hong W (2018) Neural Circuit Mechanisms of Social Behavior. Neuron 98:16-30.

Choi GB, Yim YS, Wong H, Kim S, Kim H, Kim SV, Hoeffer CA, Littman DR, Huh JR (2016) The maternal interleukin-17a pathway in mice promotes autism-like phenotypes in offspring. Science 351:933-939.

Cope EC, Wang SH, Waters RC, Gore IR, Vasquez B, Laham BJ, Gould E (2023) Activation of the CA2-ventral CA1 pathway reverses social discrimination dysfunction in Shank3B knockout mice. Nat Commun 14:1750.

Cuve HC, Gao Y, Fuse A (2018) Is it avoidance or hypoarousal? A systematic review of emotion recognition, eye-tracking, and psychophysiological studies in young adults with autism spectrum conditions. Research in Autism Spectrum Disorders 55:1-13.

Deacon RM (2006) Digging and marble burying in mice: simple methods for in vivo identification of biological impacts. Nat Protoc 1:122-124.

Defensor EB, Corley MJ, Blanchard RJ, Blanchard DC (2012) Facial expressions of mice in aggressive and fearful contexts. Physiol Behav 107:680-685.

Dolensek N, Gehrlach DA, Klein AS, Gogolla N (2020) Facial expressions of emotion states and their neuronal correlates in mice. Science 368:89-94.

Drimalla H, Baskow I, Behnia B, Roepke S, Dziobek I (2021) Imitation and recognition of facial emotions in autism: a computer vision approach. Mol Autism 12:27.

Dunbar RI (2010) The social role of touch in humans and primates: behavioural function and neurobiological mechanisms. Neurosci Biobehav Rev 34:260-268.

Ebbesen CL, Froemke RC (2021) Body language signals for rodent social communication. Curr Opin Neurobiol 68:91-106.
Ebbesen CL, Froemke RC (2022) Automatic mapping of multiplexed social receptive fields by deep learning and GPU-accelerated 3D videography. Nat Commun 13:593.
Estes ML, McAllister AK (2016) Maternal immune activation: Implications for neuropsychiatric disorders. Science 353:772-777.
Foss-Feig JH, Heacock JL, Cascio CJ (2012) Tactile Responsiveness Patterns and Their Association with Core Features in Autism Spectrum Disorders. Res Autism Spectr Disord 6:337-344.
Fukuyama H, Kumagaya SI, Asada K, Ayaya S, Kato M (2017) Autonomic versus perceptual accounts for tactile hypersensitivity in autism spectrum disorder. Sci Rep 7:8259.
Garay PA, Hsiao EY, Patterson PH, McAllister AK (2013) Maternal immune activation causes age- and region-specific changes in brain cytokines in offspring throughout development. Brain Behav Immun 31:54-68.
Gehrlach DA, Dolensek N, Klein AS, Roy Chowdhury R, Matthys A, Junghänel M, Gaitanos TN, Podgornik A, Black TD, Reddy Vaka N, Conzelmann KK, Gogolla N (2019) Aversive state processing in the posterior insular cortex. Nat Neurosci 22:1424-1437.
Goel A, Cantu DA, Guilfoyle J, Chaudhari GR, Newadkar A, Todisco B, de Alba D, Kourdougli N, Schmitt LM, Pedapati E, Erickson CA, Portera-Cailliau C (2018) Impaired perceptual learning in a mouse model of Fragile X syndrome is mediated by parvalbumin neuron dysfunction and is reversible. Nat Neurosci 21:1404-1411.
Green SA, Ben-Sasson A (2010) Anxiety disorders and sensory over-responsivity in children with autism spectrum disorders: is there a causal relationship? J Autism Dev Disord 40:1495-1504.
Green SA, Hernandez LM, Bowman HC, Bookheimer SY, Dapretto M (2018) Sensory over-responsivity and social cognition in ASD: Effects of aversive sensory stimuli and attentional modulation on neural responses to social cues. Dev Cogn Neurosci 29:127-139.
Green SA, Hernandez L, Tottenham N, Krasileva K, Bookheimer SY, Dapretto M (2015) Neurobiology of Sensory Overresponsivity in Youth With Autism Spectrum Disorders. JAMA Psychiatry 72:778-786.
He CX, Cantu DA, Mantri SS, Zeiger WA, Goel A, Portera-Cailliau C (2017) Tactile Defensiveness and Impaired Adaptation of Neuronal Activity in the Fmr1 Knock-Out Mouse Model of Autism. J Neurosci 37:6475-6487.
Heilman KJ, Harden ER, Zageris DM, Berry-Kravis E, Porges SW (2011) Autonomic regulation in fragile X syndrome. Dev Psychobiol 53:785-795.
Huang T, Lin SH, Malewicz NM, Zhang Y, Goulding M, LaMotte RH, Ma Q (2019) Identifying the pathways required for coping behaviours associated with sustained pain. Nature 565:86-90.
Jennings JH, Kim CK, Marshel JH, Raffiee M, Ye L, Quirin S, Pak S, Ramakrishnan C, Deisseroth K (2019) Interacting neural ensembles in orbitofrontal cortex for social and feeding behaviour. Nature 565:645-649.
Jeon YS, Jeong D, Kweon H, Kim JH, Kim CY, Oh Y, Lee YH, Kim CH, Kim SG, Jeong JW, Kim E, Lee SH (2023) Adolescent Parvalbumin Expression in the Left Orbitofrontal Cortex Shapes Sociability in Female Mice. J Neurosci 43:1555-1571.

Joshi S, Gold JI (2020) Pupil Size as a Window on Neural Substrates of Cognition. Trends Cogn Sci 24:466-480.
Kentner AC, Bilbo SD, Brown AS, Hsiao EY, McAllister AK, Meyer U, Pearce BD, Pletnikov MV, Yolken RH, Bauman MD (2019) Maternal immune activation: reporting guidelines to improve the rigor, reproducibility, and transparency of the model. Neuropsychopharmacology 44:245-258.
Kleberg JL, Högström J, Nord M, Bölte S, Serlachius E, Falck-Ytter T (2017) Autistic Traits and Symptoms of Social Anxiety are Differentially Related to Attention to Others' Eyes in Social Anxiety Disorder. J Autism Dev Disord 47:3814-3821.
Kliemann D, Dziobek I, Hatri A, Steimke R, Heekeren HR (2010) Atypical reflexive gaze patterns on emotional faces in autism spectrum disorders. J Neurosci 30:12281-12287.
Klusek J, Martin GE, Losh M (2013) Physiological arousal in autism and fragile X syndrome: group comparisons and links with pragmatic language. Am J Intellect Dev Disabil 118:475-495.
Kourdougli N, Suresh A, Liu B, Juarez P, Lin A, Chung DT, Graven Sams A, Gandal MJ, Martinez-Cerdeno V, Buonomano DV, Hall BJ, Mombereau C, Portera-Cailliau C (2023) Improvement of sensory deficits in fragile X mice by increasing cortical interneuron activity after the critical period. Neuron.
Kushki A, Brian J, Dupuis A, Anagnostou E (2014) Functional autonomic nervous system profile in children with autism spectrum disorder. Mol Autism 5:39.
La-Vu M, Tobias BC, Schuette PJ, Adhikari A (2020) To Approach or Avoid: An Introductory Overview of the Study of Anxiety Using Rodent Assays. Front Behav Neurosci 14:145.
Langford DJ, Bailey AL, Chanda ML, Clarke SE, Drummond TE, Echols S, Glick S, Ingrao J, Klassen-Ross T, Lacroix-Fralish ML, Matsumiya L, Sorge RE, Sotocinal SG, Tabaka JM, Wong D, van den Maagdenberg AM, Ferrari MD, Craig KD, Mogil JS (2010) Coding of facial expressions of pain in the laboratory mouse. Nat Methods 7:447-449.
Lee Masson H, Pillet I, Amelynck S, Van De Plas S, Hendriks M, Op de Beeck H, Boets B (2019) Intact neural representations of affective meaning of touch but lack of embodied resonance in autism: a multi-voxel pattern analysis study. Mol Autism 10:39.
Lenschow C, Brecht M (2015) Barrel cortex membrane potential dynamics in social touch. Neuron 85:718-725.
Mammen MA, Moore GA, Scaramella LV, Reiss D, Ganiban JM, Shaw DS, Leve LD, Neiderhiser JM (2015) INFANT AVOIDANCE DURING A TACTILE TASK PREDICTS AUTISM SPECTRUM BEHAVIORS IN TODDLERHOOD. Infant Ment Health J 36:575-587.
Mathis A, Mamidanna P, Cury KM, Abe T, Murthy VN, Mathis MW, Bethge M (2018) DeepLabCut: markerless pose estimation of user-defined body parts with deep learning. Nat Neurosci 21:1281-1289.
McGlone F, Wessberg J, Olausson H (2014) Discriminative and affective touch: sensing and feeling. Neuron 82:737-755.
Mosher CP, Zimmerman PE, Fuglevand AJ, Gothard KM (2016) Tactile Stimulation of the Face and the Production of Facial Expressions Activate Neurons in the Primate Amygdala. eNeuro 3.
Nath T, Mathis A, Chen AC, Patel A, Bethge M, Mathis MW (2019) Using DeepLabCut for 3D markerless pose estimation across species and behaviors. Nat Protoc 14:2152-2176.

Orefice LL, Zimmerman AL, Chirila AM, Sleboda SJ, Head JP, Ginty DD (2016) Peripheral Mechanosensory Neuron Dysfunction Underlies Tactile and Behavioral Deficits in Mouse Models of ASDs. Cell 166:299-313.

Orefice LL, Mosko JR, Morency DT, Wells MF, Tasnim A, Mozeika SM, Ye M, Chirila AM, Emanuel AJ, Rankin G, Fame RM, Lehtinen MK, Feng G, Ginty DD (2019) Targeting Peripheral Somatosensory Neurons to Improve Tactile-Related Phenotypes in ASD Models. Cell 178:867-886.e824.

Rais M, Binder DK, Razak KA, Ethell IM (2018) Sensory Processing Phenotypes in Fragile X Syndrome. ASN Neuro 10:1759091418801092.

Reed MD, Yim YS, Wimmer RD, Kim H, Ryu C, Welch GM, Andina M, King HO, Waisman A, Halassa MM, Huh JR, Choi GB (2020) IL-17a promotes sociability in mouse models of neurodevelopmental disorders. Nature 577:249-253.

Resendez SL, Namboodiri VMK, Otis JM, Eckman LEH, Rodriguez-Romaguera J, Ung RL, Basiri ML, Kosyk O, Rossi MA, Dichter GS, Stuber GD (2020) Social Stimuli Induce Activation of Oxytocin Neurons Within the Paraventricular Nucleus of the Hypothalamus to Promote Social Behavior in Male Mice. J Neurosci 40:2282-2295.

Robertson CE, Baron-Cohen S (2017) Sensory perception in autism. Nat Rev Neurosci 18:671-684.

Rogers SJ, Ozonoff S (2005) Annotation: what do we know about sensory dysfunction in autism? A critical review of the empirical evidence. J Child Psychol Psychiatry 46:1255-1268.

Schmitt LM, Cook EH, Sweeney JA, Mosconi MW (2014) Saccadic eye movement abnormalities in autism spectrum disorder indicate dysfunctions in cerebellum and brainstem. Mol Autism 5:47.

Shin Yim Y, Park A, Berrios J, Lafourcade M, Pascual LM, Soares N, Yeon Kim J, Kim S, Kim H, Waisman A, Littman DR, Wickersham IR, Harnett MT, Huh JR, Choi GB (2017) Reversing behavioural abnormalities in mice exposed to maternal inflammation. Nature 549:482-487.

Sinclair D, Oranje B, Razak KA, Siegel SJ, Schmid S (2017) Sensory processing in autism spectrum disorders and Fragile X syndrome-From the clinic to animal models. Neurosci Biobehav Rev 76:235-253.

Stantić M, Ichijo E, Catmur C, Bird G (2022) Face memory and face perception in autism. Autism 26:276-280.

Stringer C, Pachitariu M, Steinmetz N, Reddy CB, Carandini M, Harris KD (2019) Spontaneous behaviors drive multidimensional, brainwide activity. Science 364:255.

Stuart N, Whitehouse A, Palermo R, Bothe E, Badcock N (2022) Eye Gaze in Autism Spectrum Disorder: A Review of Neural Evidence for the Eye Avoidance Hypothesis. J Autism Dev Disord.

Sullivan K, Hatton D, Hammer J, Sideris J, Hooper S, Ornstein P, Bailey D, Jr. (2006) ADHD symptoms in children with FXS. Am J Med Genet A 140:2275-2288.

Suvilehto JT, Glerean E, Dunbar RI, Hari R, Nummenmaa L (2015) Topography of social touching depends on emotional bonds between humans. Proc Natl Acad Sci U S A 112:13811-13816.

The Dutch-Belgian Fragile X Consortium (1994) Fmr1 knockout mice: A model to study fragile X mental retardation. Cell 78:23-33.

Thye MD, Bednarz HM, Herringshaw AJ, Sartin EB, Kana RK (2018) The impact of atypical sensory processing on social impairments in autism spectrum disorder. Dev Cogn Neurosci 29:151-167.
Vinck M, Batista-Brito R, Knoblich U, Cardin JA (2015) Arousal and locomotion make distinct contributions to cortical activity patterns and visual encoding. Neuron 86:740-754.
Werling DM, Geschwind DH (2013) Sex differences in autism spectrum disorders. Curr Opin Neurol 26:146-153.
Williams DL, Goldstein G, Minshew NJ (2005) Impaired memory for faces and social scenes in autism: clinical implications of memory dysfunction. Arch Clin Neuropsychol 20:1-15.
Wolfe J, Mende C, Brecht M (2011) Social facial touch in rats. Behav Neurosci 125:900-910.
Yang M, Silverman JL, Crawley JN (2011) Automated three-chambered social approach task for mice. Curr Protoc Neurosci Chapter 8:Unit 8.26.
Yang M, Mahrt EJ, Lewis F, Foley G, Portmann T, Dolmetsch RE, Portfors CV, Crawley JN (2015) 16p11.2 Deletion Syndrome Mice Display Sensory and Ultrasonic Vocalization Deficits During Social Interactions. Autism Res 8:507-521.
Yilmaz M, Meister M (2013) Rapid innate defensive responses of mice to looming visual stimuli. Curr Biol 23:2011-2015.
Yu H, Miao W, Ji E, Huang S, Jin S, Zhu X, Liu MZ, Sun YG, Xu F, Yu X (2022) Social touch-like tactile stimulation activates a tachykinin 1-oxytocin pathway to promote social interactions. Neuron 110:1051-1067.e1057.
Zampella CJ, Bennetto L, Herrington JD (2020) Computer Vision Analysis of Reduced Interpersonal Affect Coordination in Youth With Autism Spectrum Disorder. Autism Res 13:2133-2142.

a **Experimental design for head-fixed assay**

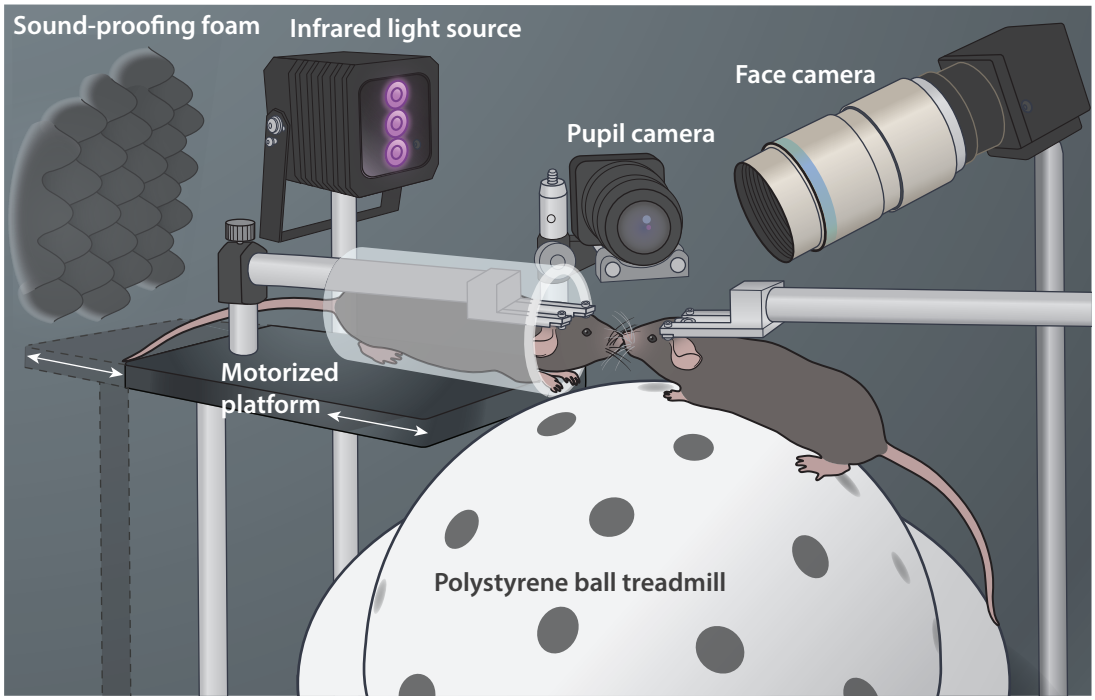

b **Types of object and social touch**

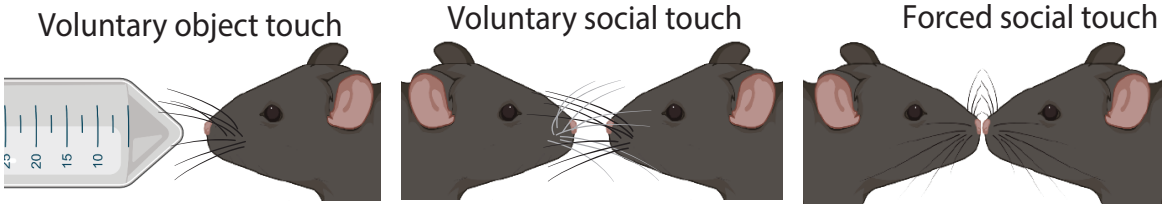

c **Experimental timeline across 2 days**

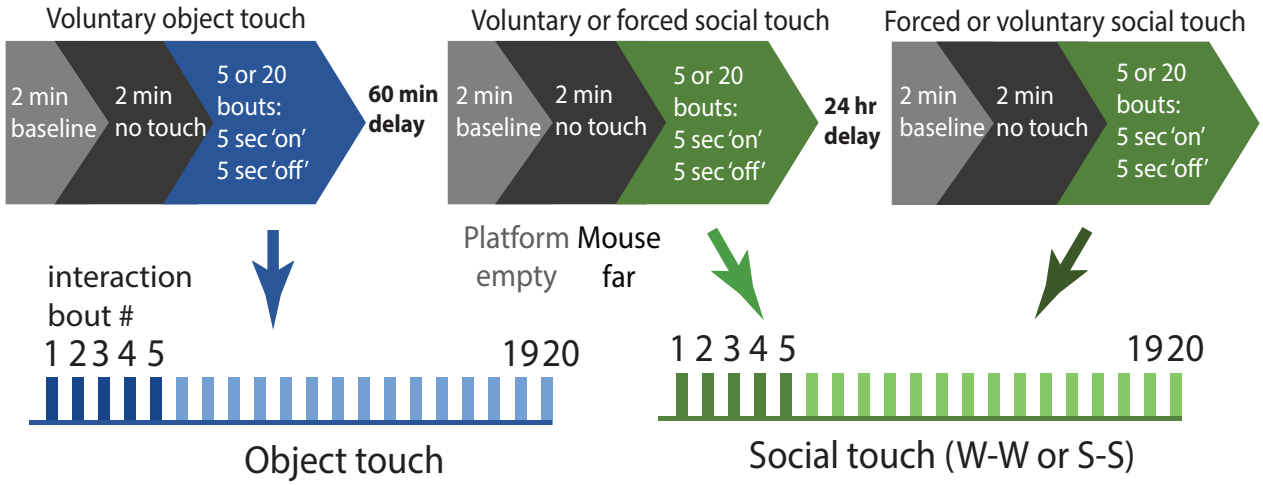

d **Camera views**

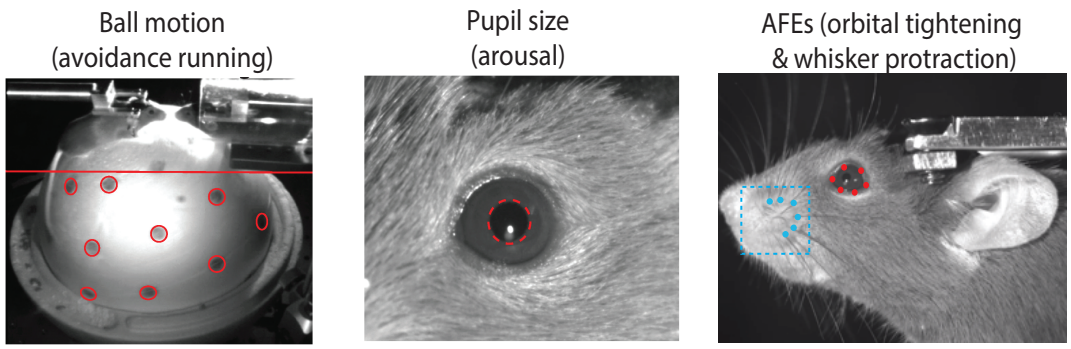

FIGURE 1

a **Interleukin-6 levels in pregnant dams at E12.5 following Poly(I:C) injection from two lots**

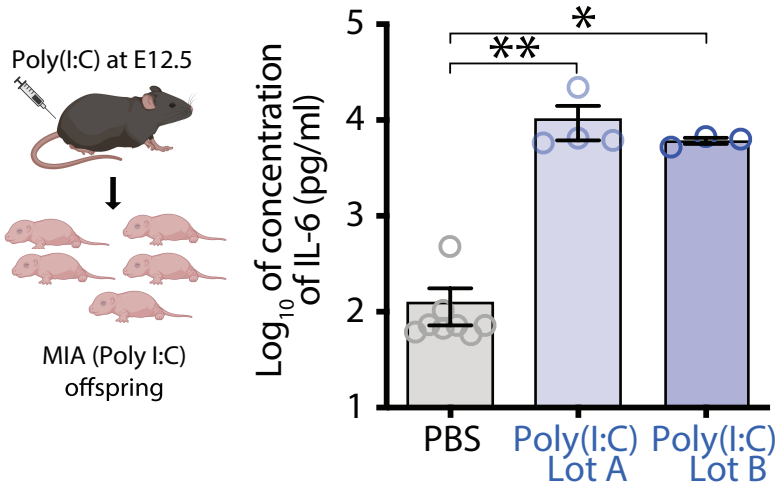

b **Offspring of Poly (I:C) dams with high IL-6 show behavioral deficits**

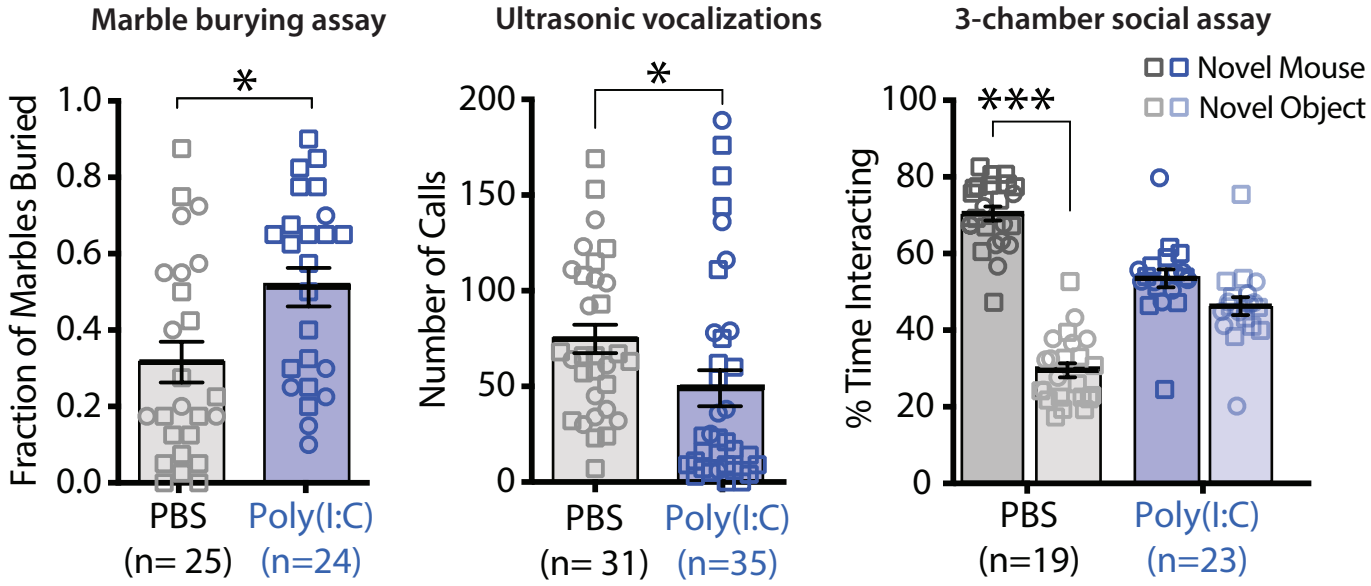

c **IL-6 levels in Poly(I:C) injected pregnant dams at E12.5 for social touch behavioral assay**

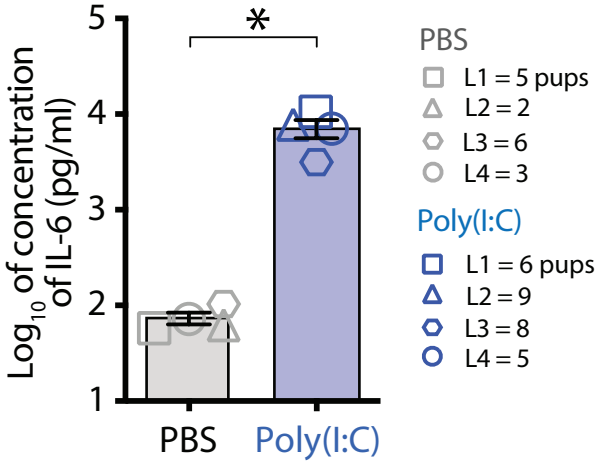

FIGURE 2

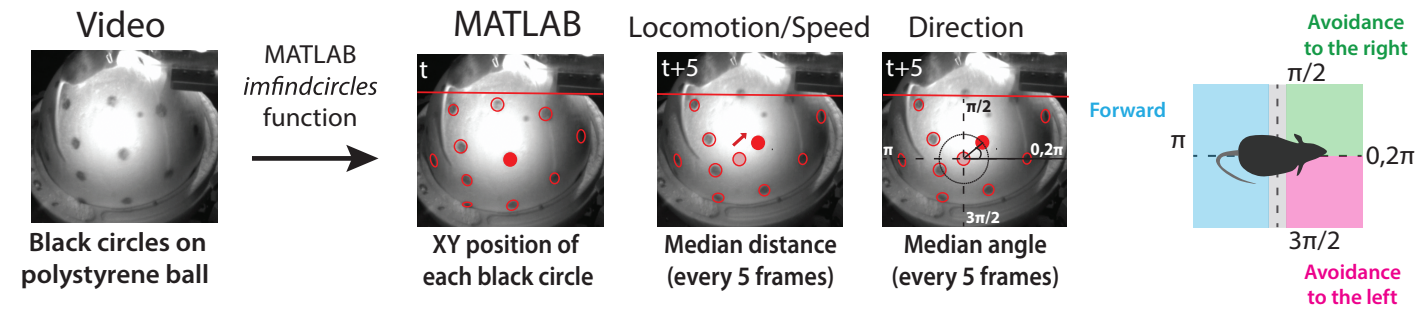
a
Running speed and direction analysis pipeline summary
Video
MATLAB
imfindcircles
function
MATLAB
Locomotion/Speed
Direction
Black circles on
polystyrene ball
XY position of
each black circle
Median distance
(every 5 frames)
Median angle
(every 5 frames)
Avoidance
to the right
Forward
Avoidance
to the left
*(All videos inspected to correct for grooming and non-directed ball movements; see Methods)

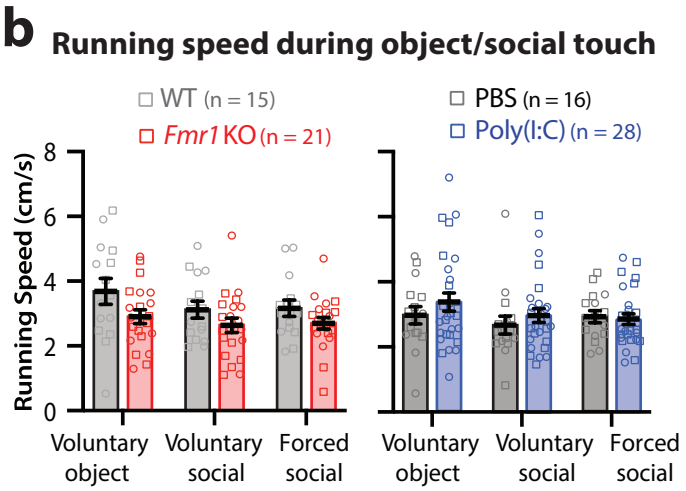
b
Running speed during object/social touch
WT (n = 15)
Fmr1 KO (n = 21)
PBS (n = 16)
Poly(I:C) (n = 28)
Running Speed (cm/s)
Voluntary object
Voluntary social
Forced social

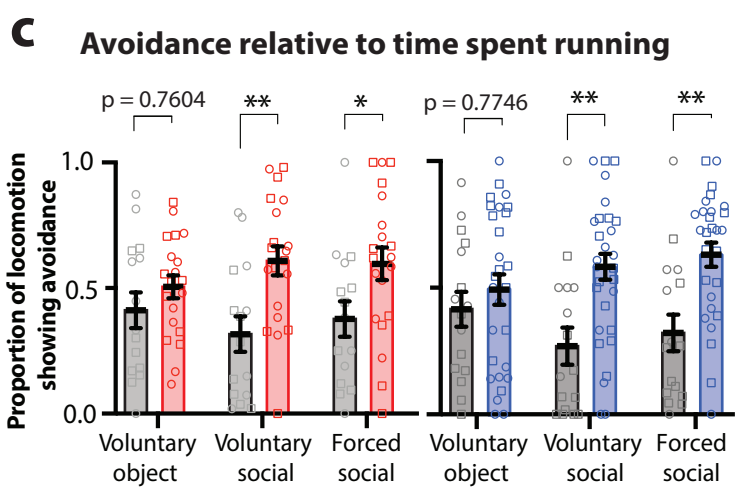
c
Avoidance relative to time spent running
p = 0.7604
**
*
p = 0.7746
**
**
Proportion of locomotion showing avoidance
Voluntary object
Voluntary social
Forced social

FIGURE 3

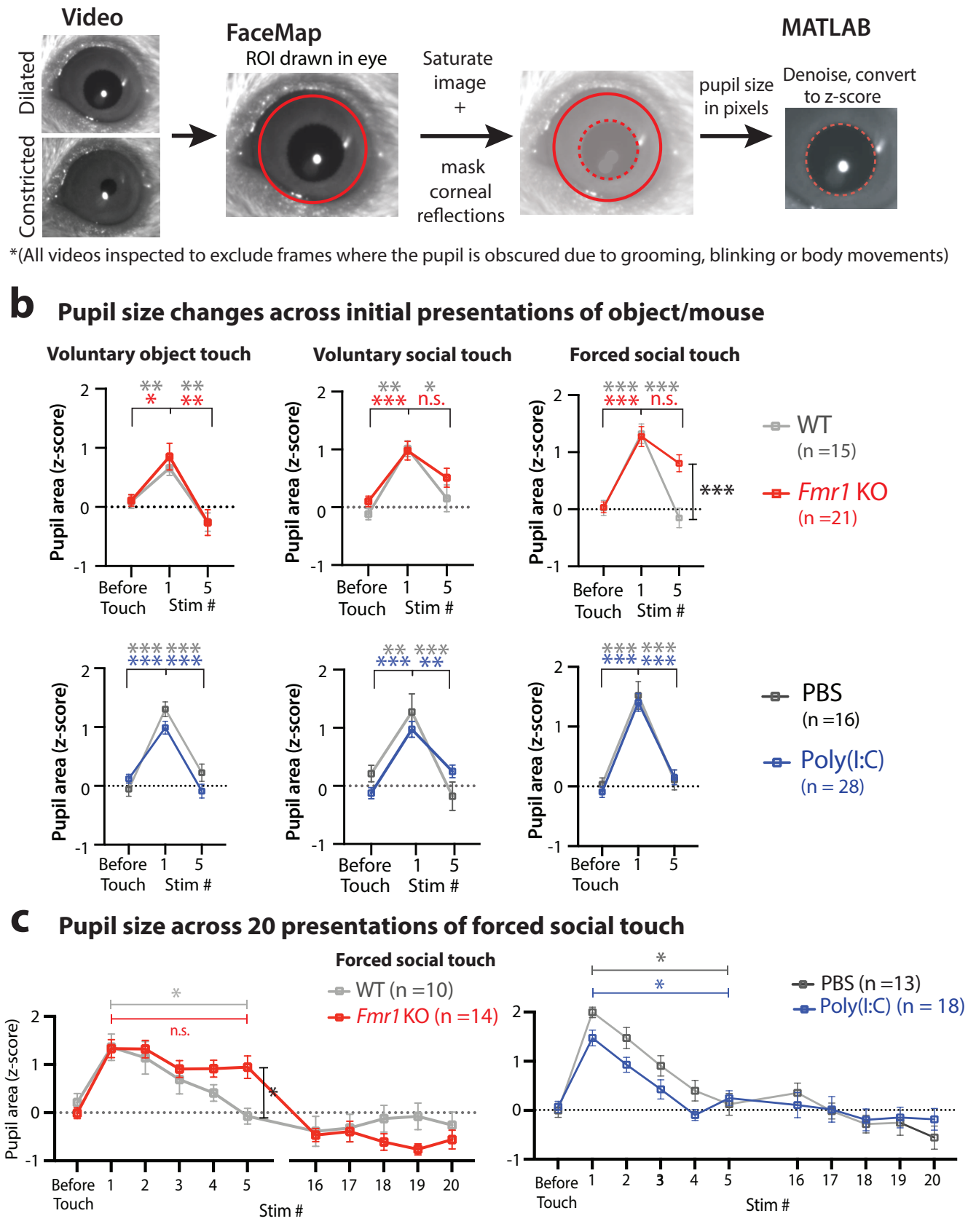
a
Pupil size analysis summary
Video
Dilated
Constricted
FaceMap
ROI drawn in eye
Saturate image +
mask corneal reflections
MATLAB
pupil size in pixels
Denoise, convert to z-score
*(All videos inspected to exclude frames where the pupil is obscured due to grooming, blinking or body movements)
b
Pupil size changes across initial presentations of object/mouse
Voluntary object touch
Voluntary social touch
Forced social touch
Pupil area (z-score)
Before Touch
Stim #
n.s.
WT
(n =15)
Fmr1 KO
(n =21)
PBS
(n =16)
Poly(I:C)
(n = 28)
c
Pupil size across 20 presentations of forced social touch
Forced social touch
WT (n =10)
Fmr1 KO (n =14)
PBS (n =13)
Poly(I:C) (n = 18)

FIGURE 4

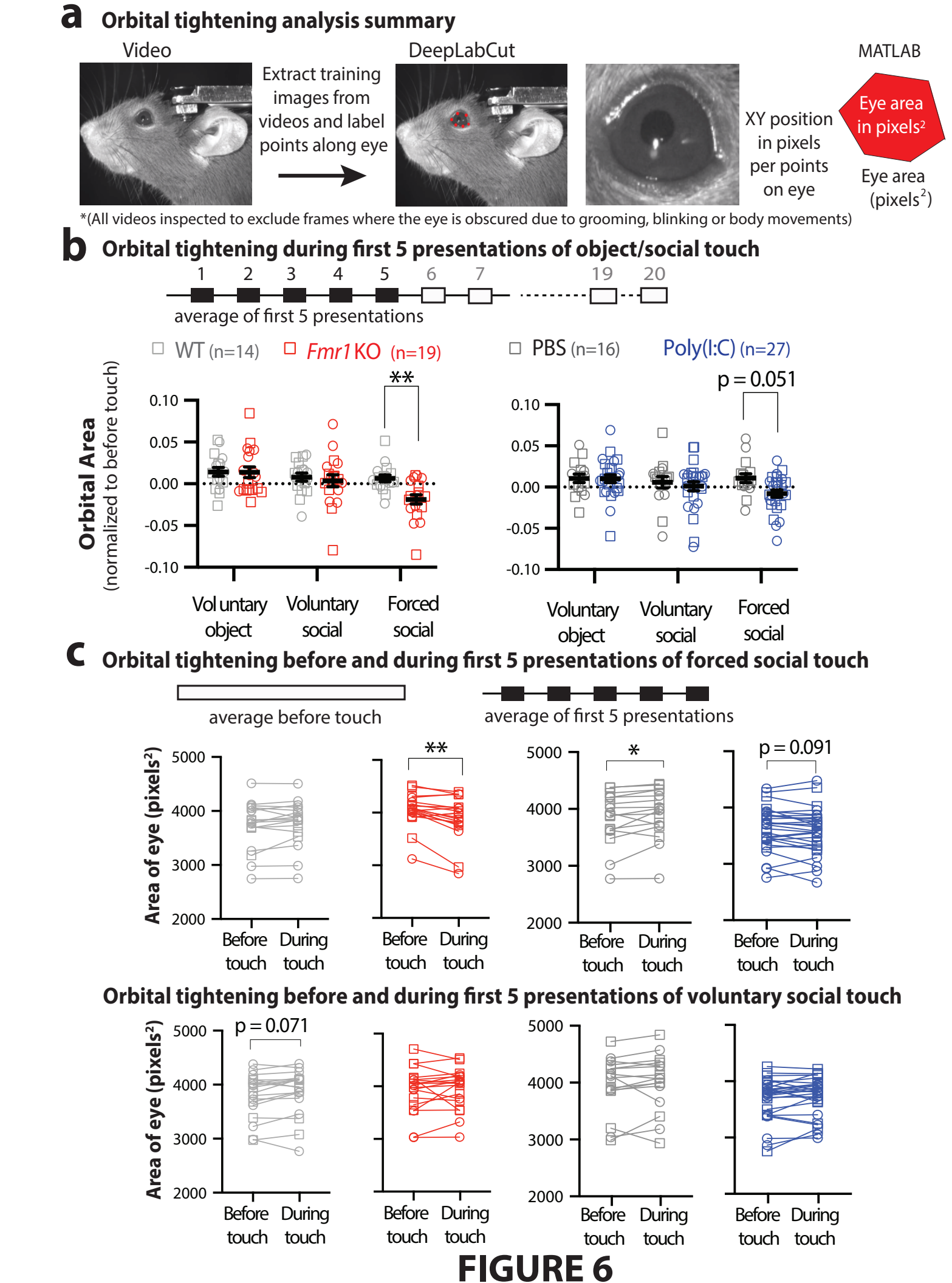
a
Orbital tightening analysis summary
Video
DeepLabCut
MATLAB
Extract training images from videos and label points along eye
XY position in pixels per points on eye
Eye area in pixels²
Eye area (pixels²)
*(All videos inspected to exclude frames where the eye is obscured due to grooming, blinking or body movements)
b
Orbital tightening during first 5 presentations of object/social touch
1 2 3 4 5 6 7 19 20
average of first 5 presentations
WT (n=14)
Fmr1 KO (n=19)
PBS (n=16)
Poly(I:C) (n=27)
Orbital Area
(normalized to before touch)
**
p = 0.051
0.10
0.05
0.00
-0.05
-0.10
Voluntary object
Voluntary social
Forced social
c
Orbital tightening before and during first 5 presentations of forced social touch
average before touch
average of first 5 presentations
Area of eye (pixels²)
5000
4000
3000
2000
**
*
p = 0.091
Before touch
During touch
Orbital tightening before and during first 5 presentations of voluntary social touch
p = 0.071

FIGURE 6

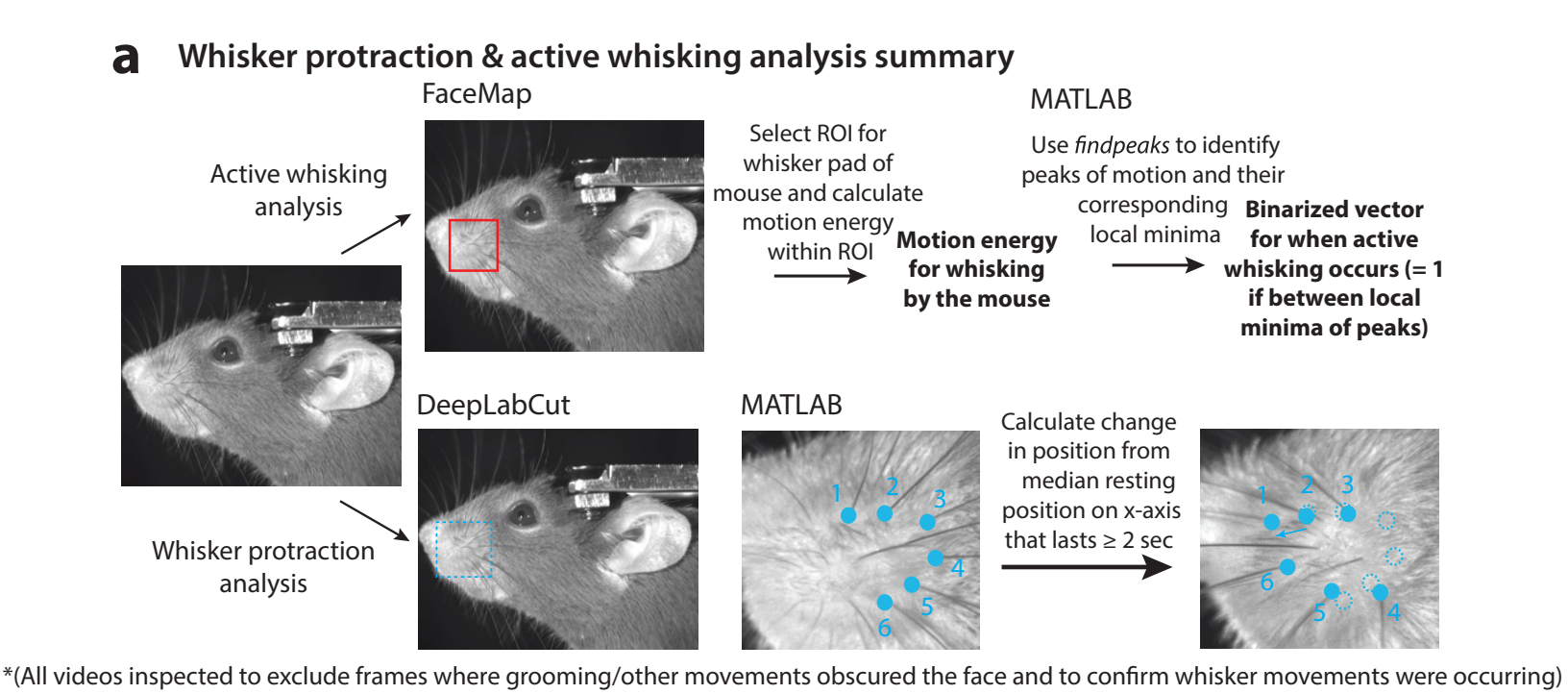
a
Whisker protraction & active whisking analysis summary
FaceMap
Active whisking analysis
Select ROI for whisker pad of mouse and calculate motion energy within ROI
Motion energy for whisking by the mouse
MATLAB
Use findpeaks to identify peaks of motion and their corresponding local minima
Binarized vector for when active whisking occurs (= 1 if between local minima of peaks)
DeepLabCut
Whisker protraction analysis
MATLAB
Calculate change in position from median resting position on x-axis that lasts ≥ 2 sec
1
2
3
4
5
6
*(All videos inspected to exclude frames where grooming/other movements obscured the face and to confirm whisker movements were occurring)

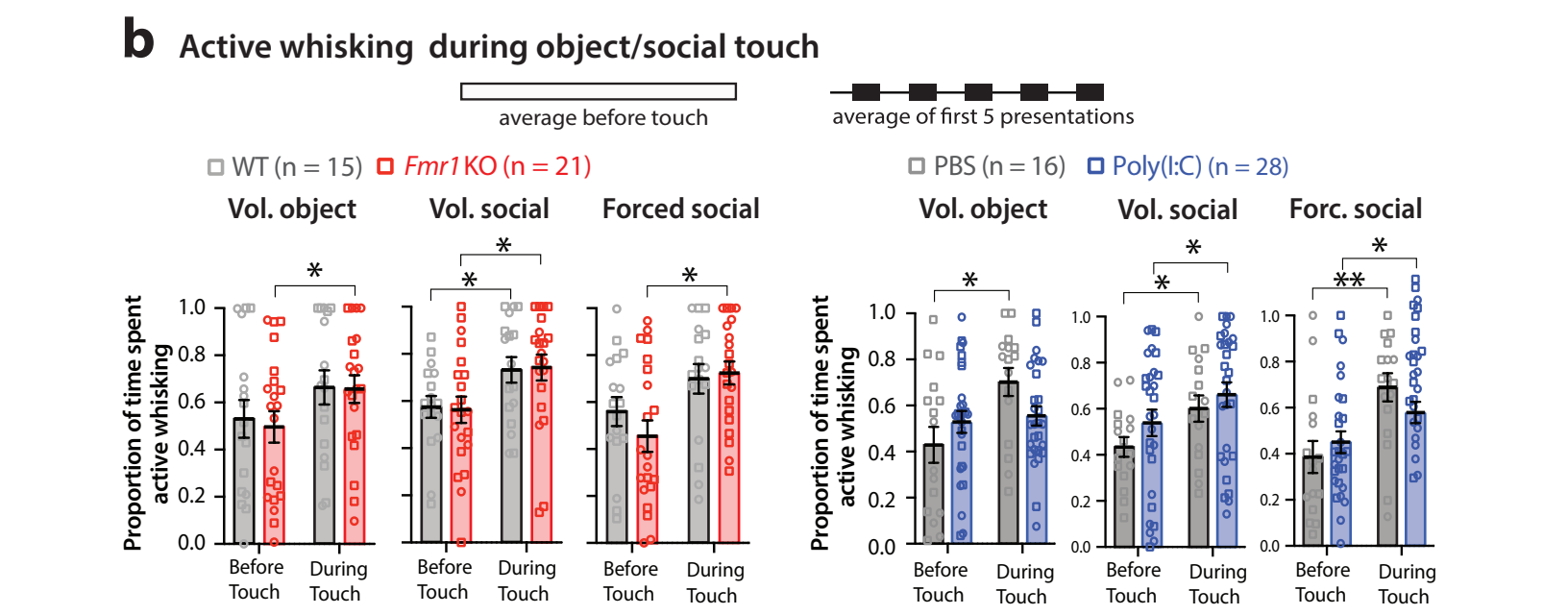
b
Active whisking during object/social touch
average before touch
average of first 5 presentations
WT (n = 15)
Fmr1 KO (n = 21)
PBS (n = 16)
Poly(I:C) (n = 28)
Vol. object
Vol. social
Forced social
Forc. social
Proportion of time spent active whisking
Before Touch
During Touch

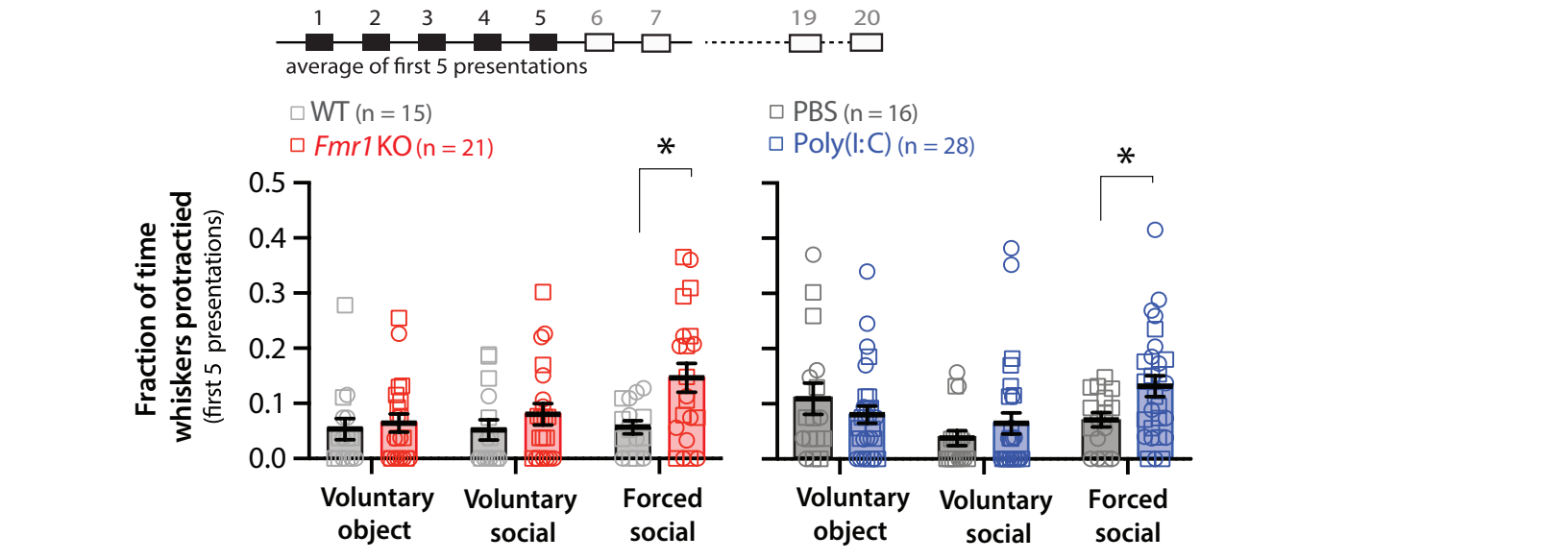
c
Prolonged aversive whisker protaction during forced social touch
1
2
3
4
5
6
7
19
20
average of first 5 presentations
WT (n = 15)
Fmr1 KO (n = 21)
PBS (n = 16)
Poly(I:C) (n = 28)
Fraction of time whiskers protracted
(first 5 presentations)
Voluntary object
Voluntary social
Forced social

FIGURE 5

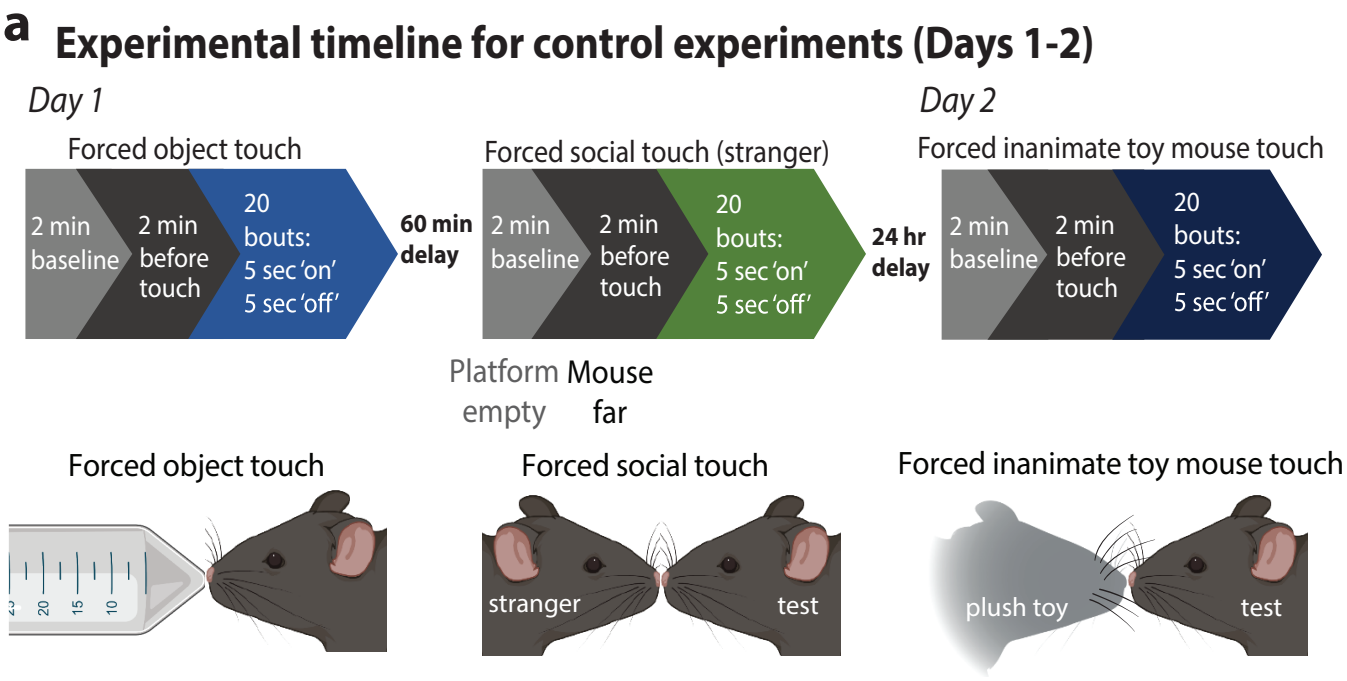
a
Experimental timeline for control experiments (Days 1-2)
Day 1
Forced object touch
2 min baseline
2 min before touch
20 bouts: 5 sec 'on' 5 sec 'off'
60 min delay
Forced social touch (stranger)
2 min baseline
2 min before touch
20 bouts: 5 sec 'on' 5 sec 'off'
24 hr delay
Day 2
Forced inanimate toy mouse touch
2 min baseline
2 min before touch
20 bouts: 5 sec 'on' 5 sec 'off'
Platform Mouse
empty far
Forced object touch
Forced social touch
stranger
test
Forced inanimate toy mouse touch
plush toy
test

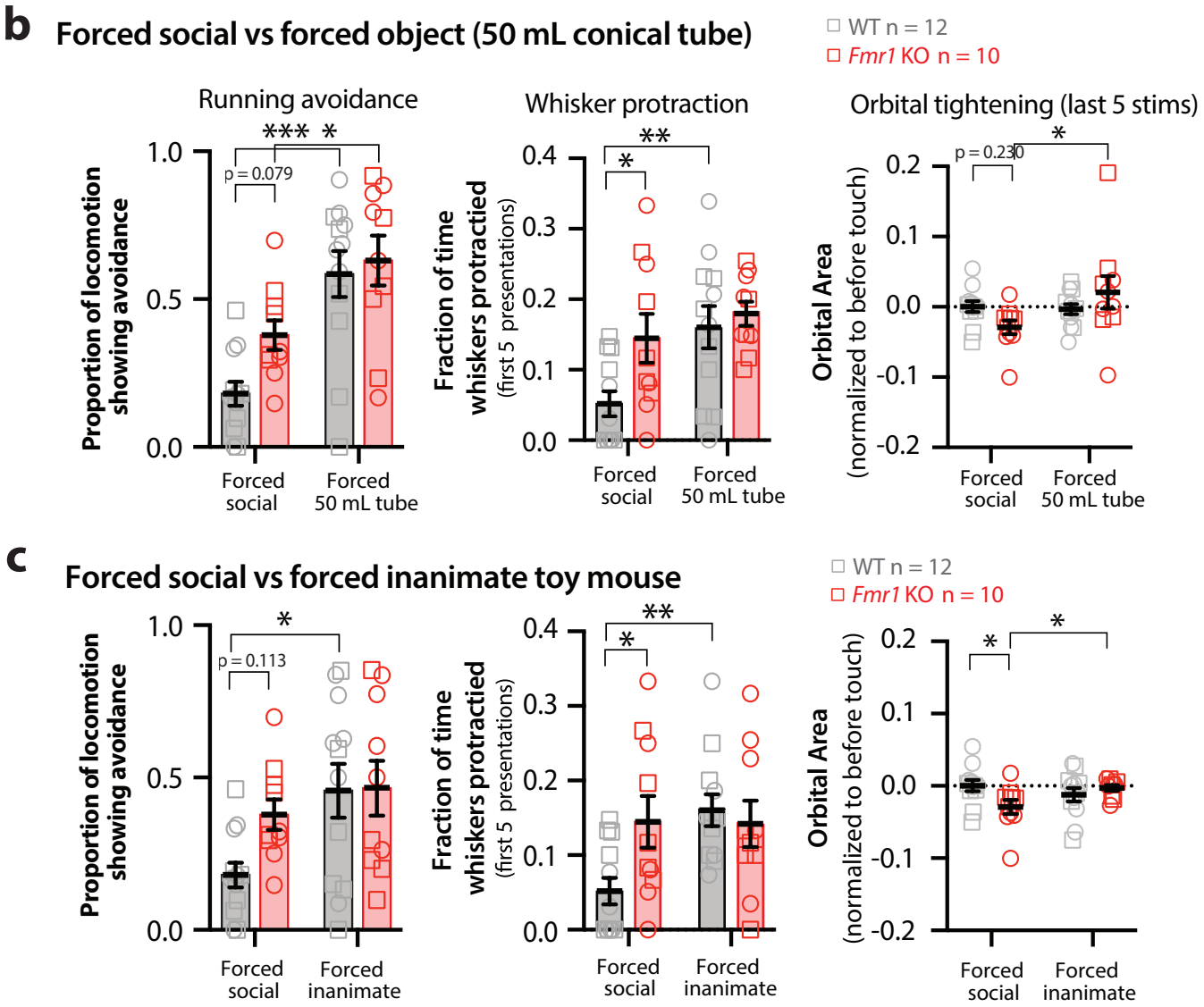
b
Forced social vs forced object (50 mL conical tube)
WT n = 12
Fmr1 KO n = 10
Running avoidance
Proportion of locomotion showing avoidance
p = 0.079
Forced social
Forced 50 mL tube
Whisker protraction
Fraction of time whiskers protracted (first 5 presentations)
Forced social
Forced 50 mL tube
Orbital tightening (last 5 stims)
Orbital Area (normalized to before touch)
p = 0.230
Forced social
Forced 50 mL tube
c
Forced social vs forced inanimate toy mouse
WT n = 12
Fmr1 KO n = 10
Proportion of locomotion showing avoidance
p = 0.113
Forced social
Forced inanimate
Fraction of time whiskers protracted (first 5 presentations)
Forced social
Forced inanimate
Orbital Area (normalized to before touch)
Forced social
Forced inanimate

FIGURE 7

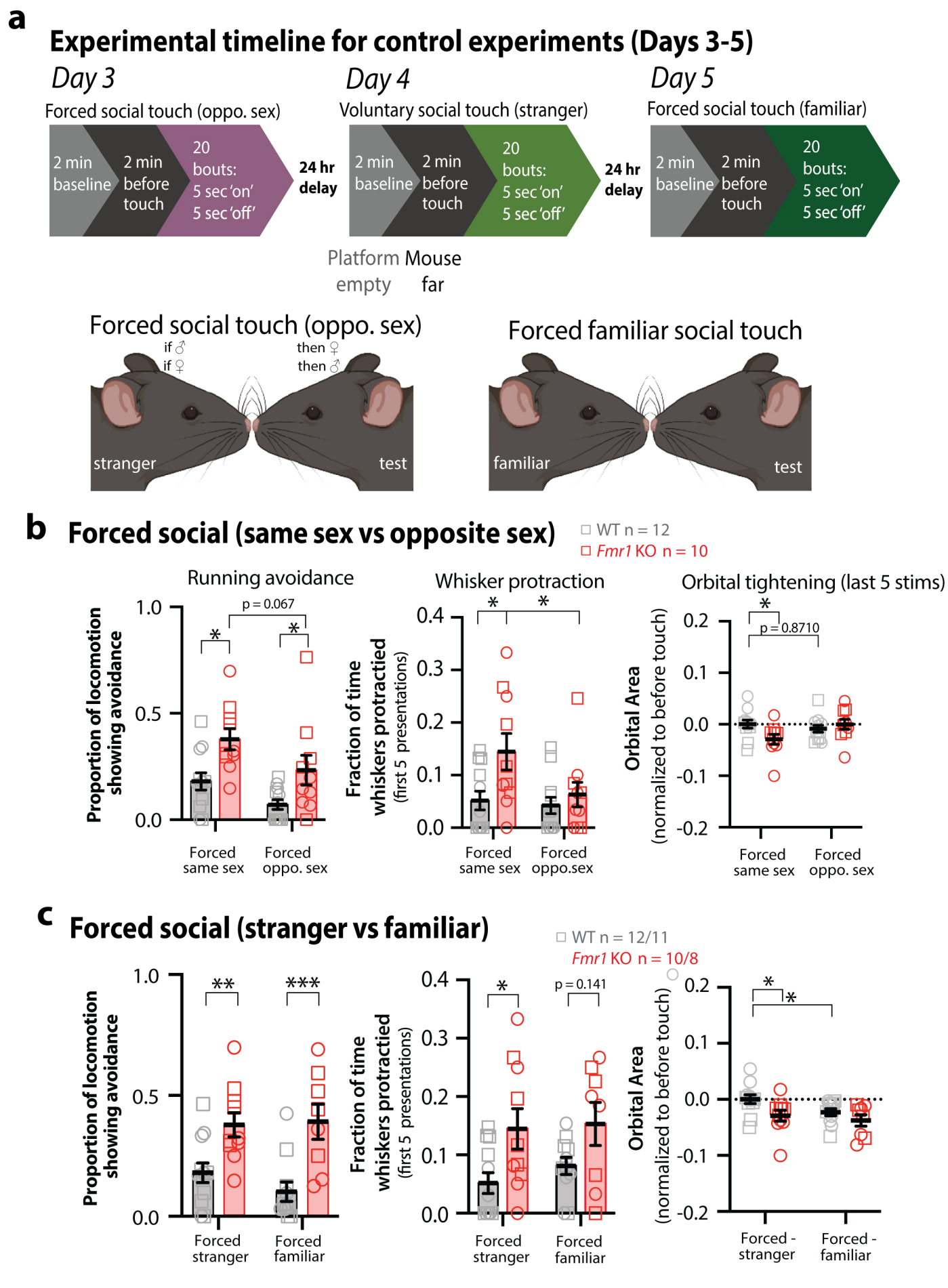
a
Experimental timeline for control experiments (Days 3-5)
Day 3
Forced social touch (oppo. sex)
2 min baseline
2 min before touch
20 bouts: 5 sec 'on' 5 sec 'off'
24 hr delay
Day 4
Voluntary social touch (stranger)
2 min baseline
2 min before touch
20 bouts: 5 sec 'on' 5 sec 'off'
24 hr delay
Day 5
Forced social touch (familiar)
2 min baseline
2 min before touch
20 bouts: 5 sec 'on' 5 sec 'off'
Platform empty
Mouse far
Forced social touch (oppo. sex)
if ♂ if ♀
then ♀ then ♂
stranger
test
Forced familiar social touch
familiar
test
b
Forced social (same sex vs opposite sex)
WT n = 12
Fmr1 KO n = 10
Running avoidance
Proportion of locomotion showing avoidance
p = 0.067
Forced same sex
Forced oppo. sex
Whisker protraction
Fraction of time whiskers protracted (first 5 presentations)
Forced same sex
Forced oppo.sex
Orbital tightening (last 5 stims)
Orbital Area (normalized to before touch)
p = 0.8710
Forced same sex
Forced oppo. sex
c
Forced social (stranger vs familiar)
WT n = 12/11
Fmr1 KO n = 10/8
Proportion of locomotion showing avoidance
Forced stranger
Forced familiar
Fraction of time whiskers protracted (first 5 presentations)
p = 0.141
Forced stranger
Forced familiar
Orbital Area (normalized to before touch)
Forced - stranger
Forced - familiar

FIGURE 8